

# Ethylene Polymerization with Dimeric Zirconium and Hafnium Silsesquioxane Complexes

Robbert Duchateau,<sup>\*,†</sup> Hendrikus C. L. Abbenhuis,<sup>†</sup> Rutger A. van Santen,<sup>†</sup>  
Auke Meetsma,<sup>‡</sup> Sven K.-H. Thiele,<sup>§</sup> and Maurits F. H. van Tol<sup>§</sup>

*Schuit Institute of Catalysis, Eindhoven University of Technology, P.O. Box 513, 5600 MB Eindhoven, The Netherlands, University of Groningen, Nijenborgh 4, 9747 AG Groningen, The Netherlands, and DSM Research B.V., P.O. Box 18, 6160 MD Geleen, The Netherlands*

Received August 12, 1998

Treatment of the silanol ( $(\text{C}_5\text{H}_9)_7\text{Si}_8\text{O}_{12}(\text{OH})$ ) with  $\text{Cp}''\text{Ti}(\text{CH}_2\text{Ph})_3$  ( $\text{Cp}'' = 1,3\text{-C}_5\text{H}_3(\text{SiMe}_3)_2$ ) or  $\text{TiCl}_4$  selectively affords the mono(silsesquioxane) complexes  $\text{Cp}''[(\text{C}_5\text{H}_9)_7\text{Si}_8\text{O}_{13}]\text{Ti}(\text{CH}_2\text{Ph})_2$  (**1**) and  $[(\text{C}_5\text{H}_9)_7\text{Si}_8\text{O}_{13}]\text{TiCl}_3$  (**2**), respectively, while with  $\text{M}(\text{CH}_2\text{Ph})_4$  ( $\text{M} = \text{Ti, Zr, Hf}$ ) mixtures of products were obtained. When the disilanol  $(\text{C}_5\text{H}_9)_7\text{Si}_7\text{O}_9(\text{OSiMe}_3)(\text{OH})_2$  is reacted with  $\text{M}(\text{CH}_2\text{Ph})_4$  ( $\text{M} = \text{Ti, Zr}$ ), the bis(silsesquioxane) complexes  $[(\text{C}_5\text{H}_9)_7\text{Si}_7\text{O}_{11}(\text{OSiMe}_3)]_2\text{M}$  ( $\text{M} = \text{Ti}$  (**3**),  $\text{Zr}$  (**4**),  $\text{Zr} \cdot 2\text{THF}$  (**5**)) are formed exclusively. With  $(\text{PhCH}_2)_2\text{ZrCl}_2 \cdot \text{OEt}_2$  as precursor, the mono(silsesquioxane) complex  $[(\text{C}_5\text{H}_9)_7\text{Si}_7\text{O}_{11}(\text{OSiMe}_3)]\text{ZrCl}_2 \cdot 2\text{THF}$  (**6**) can be isolated.  $\text{M}(\text{CH}_2\text{Ph})_4$  ( $\text{M} = \text{Ti, Zr, Hf}$ ) reacts smoothly with the tris(silanol)  $(\text{C}_5\text{H}_9)_7\text{Si}_7\text{O}_9(\text{OH})_3$  (**III**), giving the metallasilsesquioxane benzyl species,  $\{[(\text{C}_5\text{H}_9)_7\text{Si}_7\text{O}_{12}]\text{MCH}_2\text{Ph}\}_n$  ( $\text{M} = \text{Ti}$ ,  $n = 1$  (**7**);  $\text{M} = \text{Zr}$ ,  $n = 2$  (**8**);  $\text{M} = \text{Hf}$ ,  $n = 2$  (**9**)). Compounds **5** and **8** have been characterized by X-ray analysis. Dimer **8** consists of a zwitterionic-like structure with two electronically different metal sites.  $\text{M}-\text{C}$  bond hydrogenolysis of **8** and **9** affords the corresponding hydrides, which are active  $\alpha$ -olefin hydrogenation catalysts. Without cocatalyst, the neutral dimers **8** and **9** are poor, though active ethylene polymerization catalysts (activity:  $(5-10) \times 10^3$  g PE/(mol·h)). Addition of  $\text{B}(\text{C}_6\text{F}_5)_3$  affords the cationic, mono(benzyl) complexes  $\{[(\text{C}_5\text{H}_9)_7\text{Si}_7\text{O}_{12}]_2\text{M}_2(\text{CH}_2\text{Ph})\}^{(+)}$  ( $\text{M} = \text{Zr, Hf}$ ): single-site catalysts (activity:  $(2-8) \times 10^6$  g PE/(mol·h)) that are considerably more active than the neutral **8** and **9**. Whereas titanasilsesquioxanes **3** and **7** do not react with THF, the corresponding zirconasilsesquioxanes **4** and **8** form bis(THF) adducts,  $[(\text{C}_5\text{H}_9)_7\text{Si}_7\text{O}_{11}(\text{OSiMe}_3)]_2\text{Zr} \cdot 2\text{THF}$  (**5**) and  $[(\text{C}_5\text{H}_9)_7\text{Si}_7\text{O}_{12}]\text{ZrCH}_2\text{Ph} \cdot 2\text{THF}$  (**10**), which suggests that the titanium complexes are less electrophilic than the zirconium ones. Accordingly, the titanium complex **7** does not react with dihydrogen and is inactive in ethylene polymerization.

## Introduction

Although metallocenes are among the most active olefin polymerization catalysts known to date,<sup>1</sup> their commercial use remains limited. The industrial applicability of homogeneous metallocene based olefin polymerization catalysts is not so much limited by the activity or selectivity of the catalyst but more due to restrictions such as poor polymer morphology and the necessity of large quantities of the cocatalyst methylalumoxane (MAO), which makes processing of the polymer difficult and expensive. These problems can partly be overcome by using immobilized catalysts.<sup>2</sup> For example, morphology control by replication can lead to uniform polymer particles with a high bulk density,<sup>3</sup> whereas site isolation reduces bimolecular deactivation

processes as a result of which the necessary amount of MAO can be reduced.<sup>4</sup> Metallocenes physisorbed onto MAO-pretreated supports yield systems that resemble their unsupported analogues.<sup>5a,b</sup> However, a drawback of these systems is that leaching remains a problem and the activities are rather low. On the other hand, silica- or alumina-grafted early transition metal complexes are much more robust with respect to leaching and do not need to be activated by a cocatalyst.<sup>2b,g,5c</sup> Although recent studies show that oxide-grafted organometallic complexes can be quite uniform in structure, reactivity,

\* Corresponding author. E-mail: R.Duchateau@tue.nl. Fax: +31 40 245 5054.

<sup>†</sup> Eindhoven University of Technology.

<sup>‡</sup> University of Groningen.

<sup>§</sup> DSM Research B.V.

(1) (a) Kaminsky, W.; Miri, M.; Sinn, H.; Woldt, R. *Makromol. Chem., Rapid. Commun.* **1983**, *4*, 417. (b) Spaleck, W.; Küber, F.; Winter, A.; Rohrmann, J.; Bachmann, B.; Antberg, M.; Dolle, V.; Paulus, E. F. *Organometallics* **1994**, *13*, 954. (c) Sinclair, K. B.; Wilson, R. B. *Chem. Ind.* **1994**, 857. (d) Hackmann, M.; Rieger, B. *CATTECH* **1997**, *2*, 79.

(2) For example see: (a) Zakharov, V. A.; Yermakov, Y. I. *Catal. Rev.-Sci. Eng.* **1979**, *19*, 67. (b) Collette, J. W.; Tullock, C. W. U.S. Patent 4,298,722 (Du Pont), 1981. (c) Keii, T.; Soga, K., Eds. *Catalytic Polymerization of Olefins, Studies in Surface Science and Catalysis*; Elsevier: New York, 1986. (d) Kaminsky, W.; Sinn, H., Eds. *Transition Metals and Organometallics as Catalysts for Olefin Polymerization*; Springer-Verlag: New York, 1988. (e) Marks, T. J. *Acc. Chem. Res.* **1992**, *25*, 57. (f) Marsden, C. E. *Plast., Rubber Compos. Process. Appl.* **1994**, *21*, 193. (g) *Proceedings of SPO '96* **1996**, 283. (h) Olabisi, O.; Atiquilla, M.; Kaminsky, W. *Makromol. Chem. Phys.* **1997**, *C37*(3), 519, and references therein.

(3) For example see: Hungenberg, K. H.; Kerth, J.; Langhauser, F.; Marczinke, B.; Schlund, R. In *Ziegler Catalysts*; Fink, G., Mülhaupt, R., Brintzinger, H. H., Eds.; Springer-Verlag: New York, 1995; Chapter 20.

(4) Chien, J. C. W.; He, D. *J. Polym. Sci.: Part A: Polym. Chem.* **1991**, 1603.

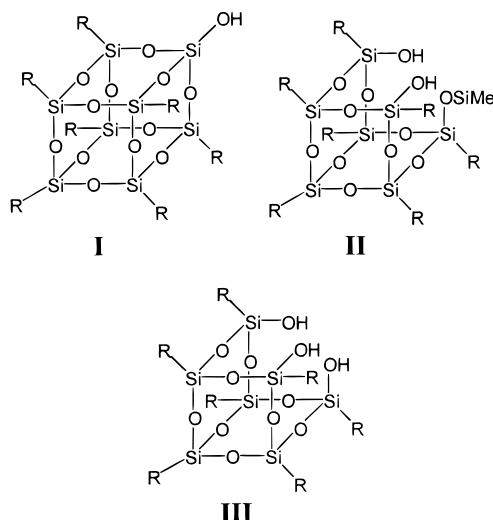
and distribution, their exact structure often remains a subject of debate.<sup>6</sup> Despite advances in spectroscopic, physical, and chemical techniques, investigation of the processes taking place at these catalyst surfaces remains inherently difficult.<sup>7</sup> As a consequence, efforts have been undertaken to develop homogeneous model systems to mimic silica surface metal complexes. One sophisticated example in which homogeneous model systems have proven to be very useful for the understanding of reactions taking place at surfaces involves silsesquioxanes. Elegant work of Feher et al.<sup>8</sup> has demonstrated that partly condensed silsesquioxanes are suitable structural models for a variety of surface sites ranging from isolated silanols to silanol nests, as found in silicas and zeolitic materials. The power of these model systems arises from the fact that standard characterization techniques such as solution NMR spectroscopy provide crucial information that cannot be obtained from the corresponding heterogeneous systems. In addition, the high uniform character of the silsesquioxanes provides an excellent possibility to fine-tune synthetic procedures to anchor the metal complex to the support. Recent results have shown that (metal)silsesquioxanes are also very suitable to perform quantum mechanical calculations which can lead to reliable predictions for the corresponding silica-supported systems.<sup>9b</sup>

Our interest in silsesquioxane chemistry is aimed at developing homogeneous group 4 metal silsesquioxane complexes and to compare the catalytic activity of these metallasilsesquioxanes with that of corresponding heterogeneous catalysts. We report here the synthesis of group 4 metal silsesquioxane complexes and their use as olefin hydrogenation and polymerization catalysts. These results provide insight into some very interesting mechanistic aspects of silsesquioxane-based Ziegler–Natta catalysts.

## Results and Discussion

**Synthesis of Silsesquioxane Group 4 Metal Complexes.** Three different silsesquioxanes, each representing a different type of surface silanol site, were selected for our investigation (Scheme 1): the monodentate cube-octameric spherosilicate  $(\text{-C}_5\text{H}_9)_7\text{Si}_8\text{O}_{12}(\text{OH})$  (**I**), re-

**Scheme 1**



cently synthesized in our group,<sup>9</sup> and Feher's disilanol  $(\text{-C}_5\text{H}_9)_7\text{Si}_7\text{O}_9(\text{OSiMe}_3)(\text{OH})_2$  (**II**) and trisilanol  $(\text{-C}_5\text{H}_9)_7\text{Si}_7\text{O}_9(\text{OH})_3$  (**III**), respectively.<sup>8</sup> With these ligands available, we aimed to prepare homogeneous complexes that mimic the corresponding silica-supported group 4 metal alkyl and hydride complexes as reported by, for example, Schwartz and Basset.<sup>6b–f</sup> Since protolysis of metal precursors containing a hydrolyzable ligand is the preferred route to synthesize silica-grafted systems,<sup>6</sup> it was also the selected method for the preparation of silsesquioxane complexes.

**Silanol I.** In accordance with the grafting of group 4 metal alkyls onto partly dehydroxylated silica<sup>6</sup> and the alcoholysis with ROH (e.g., ROH =  $(\text{Me}_3\text{C})_3\text{COH}$ , 2,6- $(\text{Me}_3\text{C})_2\text{-C}_6\text{H}_3\text{OH}$ , 2,2'- $\text{CH}_2(\text{C}_6\text{H}_4\text{-4-Me-6-(CMe}_3\text{OH)})_2$ ),<sup>10</sup> introduction of silsesquioxane **I** to group 4 metal half-sandwich complexes is conveniently achieved by protolysis.<sup>9</sup> For example, as described in detail elsewhere,<sup>9</sup>  $\text{Cp}''\text{Ti}(\text{CH}_2\text{Ph})_3$  ( $\text{Cp}'' = 1,3\text{-(Me}_3\text{Si)}_2\text{C}_5\text{H}_3$ ) reacts selectively with **I** to produce the corresponding silsesquioxane complex  $\text{Cp}''[(\text{-C}_5\text{H}_9)_7\text{Si}_8\text{O}_{13}]\text{Ti}(\text{CH}_2\text{Ph})_2$  (**1**, eq 1). Similarly,  $\text{TiCl}_4$  reacts with 1 equiv of **I**, liberating HCl and affording the (silsesquioxane)titaniumtrichloride,  $[(\text{-C}_5\text{H}_9)_7\text{Si}_8\text{O}_{13}]\text{TiCl}_3$  (**2**), in good yield (eq 2).<sup>11</sup>

Surprisingly, the protolysis of **I** by homoleptic group 4 metal benzyl complexes,  $\text{M}(\text{CH}_2\text{Ph})_4$  ( $\text{M} = \text{Ti, Zr, Hf}$ ), is completely aselective. Instead of the expected product,  $[(\text{-C}_5\text{H}_9)_7\text{Si}_8\text{O}_{13}]\text{M}(\text{CH}_2\text{Ph})_3$ , only complicated product mixtures were observed containing significant amounts of the precursor  $\text{M}(\text{CH}_2\text{Ph})_4$ . Even the reaction of

(5) (a) Soga, K.; Kaminsky, W. *Makromol. Chem., Rapid Commun.* **1992**, *13*, 221. (b) Soga, K.; Kaminsky, W. *Makromol. Chem.* **1993**, *194*, 1745. (c) Kaminsky, W.; Renner, F. *Makromol. Chem., Rapid Commun.* **1993**, *14*, 239.

(6) (a) Ballard, D. G. H. *Adv. Catal.* **1973**, *23*, 263. (b) Schwartz, J.; Ward, M. D. *J. Mol. Catal.* **1980**, *8*, 465. (c) King, S. A.; Schwartz, J. *Inorg. Chem.* **1991**, *30*, 3771. (d) Scott, S. L.; Basset, J.-M.; Niccolai, G. P.; Santini, C. C.; Candy, J.-P.; Lecuyer, C.; Quignard, F.; Choplin, A. *New J. Chem.* **1994**, *18*, 115. (e) Vidal, V.; Théolier, A.; Thivolle-Cazat, J.; Basset, J.-M.; Corker, J. *J. Am. Chem. Soc.* **1996**, *118*, 4595. (f) Quignard, F.; Lecuyer, C.; Choplin, A.; Basset, J.-M. *J. Chem. Soc., Dalton Trans.* **1994**, 1153. (g) Ajjou, J. A.; Scott, S. *Organometallics* **1997**, *16*, 86. (h) Bade, O. M.; Blom, R.; Ystenes, M. *Organometallics* **1998**, *17*, 2524. (i) Theopold, K. H. *Eur. J. Inorg. Chem.* **1998**, *15*, and references therein.

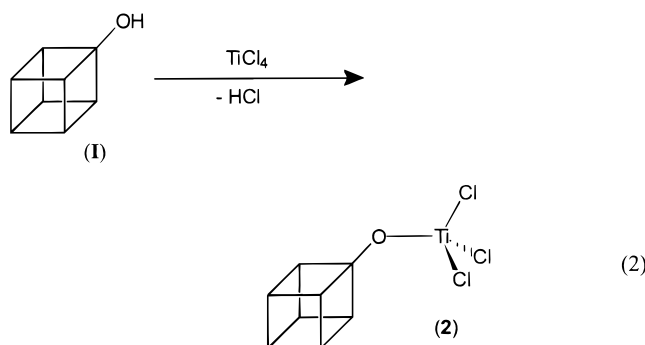
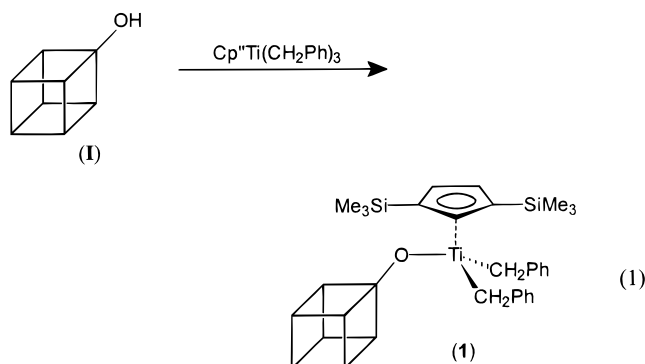
(7) (a) Tamura, K. *Dynamic Heterogeneous Catalysis*; Academic Press: New York, 1978. (b) Delgass, W. N.; Haller, G. L.; Kellerman, R.; Lunford, J. H. *Spectroscopy in Heterogeneous Catalysis*; Academic Press: New York, 1979. (c) Delannay, F. *Characterization of Heterogeneous Catalysts*; Marcel Dekker: New York, 1984. (d) Fu, S. L.; Rosynek, M. P.; Lunsford, J. *Langmuir* **1991**, *7*, 1179. (e) Schnellback, M.; Köhler, F. H.; Blümel, J. *J. Organomet. Chem.* **1996**, *520*, 227.

(8) (a) Feher, F. J.; Newman, D. A.; Walzer, J. F. *J. Am. Chem. Soc.* **1989**, *111*, 1741. (b) Feher, F. J.; Newman, D. A. *J. Am. Chem. Soc.* **1990**, *112* (2), 1931. (c) Feher, F. J.; Budzichowski, T. A.; Blanski, R. L.; Weller, K. J.; Ziller, J. W. *Organometallics* **1991**, *10*, 2526.

(9) (a) Duchateau, R.; Abbenhuis, H. C. L.; van Santen, R. A.; Thiele, S. K.-H.; van Tol, M. F. H. *Organometallics*, in press. (b) Duchateau, R.; Cremer, U.; Harmsen, R.; Mohamud, S.; Abbenhuis, H. C. L.; van Santen, R. A.; Meetsma, A.; Thiele, S. K.-H.; van Tol, M. F. H. Manuscript in preparation.

(10) (a) Lubben, T. V.; Wolczanski, P. T.; Van Duyne, G. D. *Organometallics* **1984**, *3*, 977. (b) Latesky, S. L.; McMullen, A. K.; Niccolai, G. P.; Rothwell, I. P. *Organometallics* **1985**, *4*, 902. (c) Okuda, J.; Fokken, S.; Kang, H.-C.; Massa, W. *Chem. Ber.* **1995**, *128*, 221.

(11) Similar dehydrochlorination reactions have been reported for both homogeneous and heterogeneous systems. For example: (a) Park, J. R.; Shiono, T.; Soga, K. *Macromolecules* **1992**, *25*, 521. (b) Nomura, K.; Naga, N.; Miki, M.; Ynagi, K.; Imai, A. *Organometallics* **1998**, *17*, 2152.

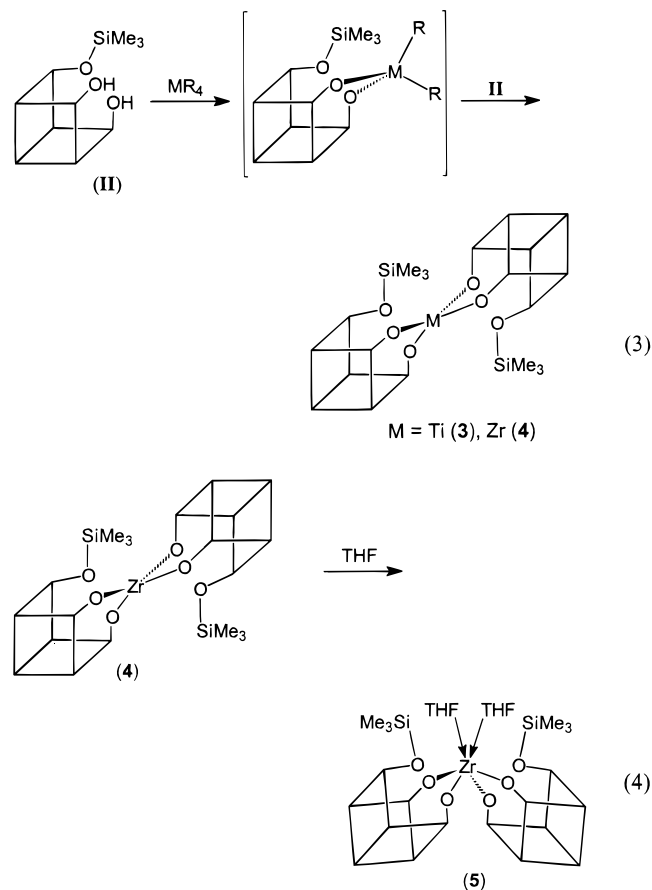


$\text{M}(\text{CH}_2\text{Ph})_4$  with 2 or 3 equiv of **I** proved unsuccessful, resulting in a mixture of products including  $\text{M}(\text{CH}_2\text{Ph})_4$ . The formation of these product mixtures indicates that the rate of protolysis for the intermediate silsesquioxane metal benzyl complexes is at least of the same order as for  $\text{M}(\text{CH}_2\text{Ph})_4$ . This contrasts with the mono(silsesquioxane) complexes  $\text{Cp}^*[(c\text{-C}_5\text{H}_9)_7\text{Si}_8\text{O}_{13}]\text{Ti}(\text{CH}_2\text{Ph})_2$  and  $[(c\text{-C}_5\text{H}_9)_7\text{Si}_8\text{O}_{13}]\text{TiCl}_3$  (**2**), which refuse to react with another equivalent of **I** even under forced conditions (toluene, reflux).

The reaction of  $\text{M}(\text{CH}_2\text{Ph})_4$  with silanol **I** is considerably faster than with alcohols. Whereas the reaction of  $\text{Zr}(\text{CH}_2\text{Ph})_4$  with **I** is nearly instantaneous at room temperature, protolysis of tritoxH  $((\text{Me}_3\text{C})_3\text{COH})$ <sup>10a</sup> requires refluxing in benzene to proceed. With a cone angle of  $\sim 125^\circ$ ,<sup>10a</sup> tritoxH is sterically less hindered than silanol **I** (cone angle =  $148^\circ$ ).<sup>9b</sup> Hence, the observed difference in reactivity between tritox and **I** is probably electronic rather than steric in origin. This assumption is supported by results of Feher et al.,<sup>12</sup> who reported the  $[\text{Si}_8\text{O}_{12}]$  cage to be as electron-withdrawing as a  $\text{CF}_3$  group. Hence, it is justifiable to assume that silanol **I** is a stronger Brønsted acid than tritoxH, giving faster, and less selective, protolysis reactions.

**Disilanol II.** Following the reactions with silanol **I**, protolysis reactions were carried out with the disilanol  $(c\text{-C}_5\text{H}_9)_7\text{Si}_7\text{O}_9(\text{OSiMe}_3)(\text{OH})_2$  (**II**), a model for bipodal silica silanol sites. Since they are suitable model systems for Schwartz's silica-supported  $[\equiv\text{SiO}]_2\text{ZrR}_2$  ( $\text{R} = \text{H}$ , alkyl)<sup>6b,c</sup> and potential precursors for catalytic olefin polymerization, attempts were undertaken to synthesize mono(silsesquioxane) metal bis(alkyl) complexes of the type  $[(c\text{-C}_5\text{H}_9)_7\text{Si}_7\text{O}_{11}(\text{OSiMe}_3)]\text{MR}_2$ . The reaction between equimolar amounts of **II** and  $\text{M}(\text{CH}_2\text{Ph})_4$  ( $\text{M} = \text{Ti}$ , Zr) in toluene resulted selectively in a 1:1 mixture

of  $\text{M}(\text{CH}_2\text{Ph})_4$  and  $[(c\text{-C}_5\text{H}_9)_7\text{Si}_7\text{O}_{11}(\text{OSiMe}_3)]_2\text{M}$  ( $\text{M} = \text{Ti}$  (**3**), Zr (**4**), eq 3). As observed for silanol **I**, protolysis reactions of **II** are nonselective in the sense that incorporation of the second silsesquioxane ligand is faster than the first one. Although undesired in view of our goal to prepare olefin polymerization catalysts, this phenomenon is in agreement with the reported activating effect of alumina and aluminosilicate carriers on group 4 metal complexes.<sup>2,6</sup> When soluble silsesquioxanes are used instead of these solid supports, bimolecular reactions exclude isolation of reactive intermediates and inherently result in the formation of thermodynamically stable complexes such as **3** and **4** or product mixtures.



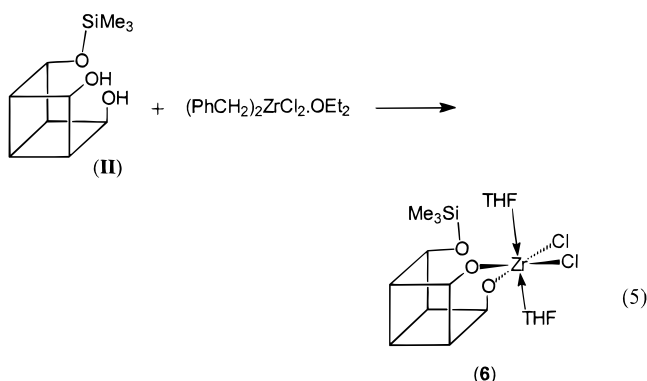
Both metallasilsesquioxane complexes **3** and **4** could be synthesized in excellent yield by treatment of toluene solutions of  $\text{M}(\text{CH}_2\text{Ph})_4$  with 2 equiv of silsesquioxane **II** (eq 3). During the course of this investigation, Crocker et al. reported the synthesis of the cyclohexyl-substituted analogue of **3**,  $[(c\text{-C}_6\text{H}_{11})_7\text{Si}_7\text{O}_{11}(\text{OSiMe}_3)]_2\text{Ti}$ , which was used as an olefin epoxidation catalyst.<sup>13</sup> Noteworthy to mention is that in the presence of THF **4** readily forms the bis(THF) adduct  $[(c\text{-C}_5\text{H}_9)_7\text{Si}_7\text{O}_{11}(\text{OSiMe}_3)]_2\text{Zr} \cdot 2\text{THF}$  (**5**, eq 4), whereas **3** refuses to react with Lewis bases (THF, MeCN). This low tendency of **3** to form Lewis base adducts cannot be explained by the difference in steric hindrance (ionic radii:  $\text{Ti}^{4+} = 0.74 \text{ \AA}$ ,  $\text{Zr}^{4+} = 0.86 \text{ \AA}$ )<sup>14</sup> for **3** and **4** alone. Hence it appears that **3** is significantly less Lewis acidic than **4** (vide infra).

Alternative routes to prepare mono(silsesquioxane) metal bis(alkyl) complexes of the type  $[(c\text{-C}_5\text{H}_9)_7\text{Si}_7\text{O}_{11}(\text{OSiMe}_3)]\text{MR}_2$  were also investigated. By treatment of

(12) (a) Feher, F. J.; Budzichowski, T. A. *J. Organomet. Chem.* **1989**, 379, 33. (b) Feher, F. J.; Tajima, T. L. *J. Am. Chem. Soc.* **1994**, 116, 2145.



(PhCH<sub>2</sub>)<sub>2</sub>ZrCl<sub>2</sub>·OEt<sub>2</sub> with disilanol (*c*-C<sub>5</sub>H<sub>9</sub>)<sub>7</sub>Si<sub>7</sub>O<sub>9</sub>-(OSiMe<sub>3</sub>)(OH)<sub>2</sub> (**II**) incorporation of a second equivalent of **II** was successfully avoided, yielding the corresponding mono(silsesquioxane) zirconium dichloride, [(*c*-C<sub>5</sub>H<sub>9</sub>)<sub>7</sub>Si<sub>7</sub>O<sub>11</sub>(OSiMe<sub>3</sub>)]ZrCl<sub>2</sub>·2THF (**6**, eq 5) in excellent yield. Alkylation of **6** is currently under investigation, although separation problems have until now prevented the isolation of well-defined products. Alternatively, the reaction of (PhCH<sub>2</sub>)<sub>2</sub>ZrCl<sub>2</sub>·OEt<sub>2</sub> with 1 equiv of the thallium salt of **II**, (*c*-C<sub>5</sub>H<sub>9</sub>)<sub>7</sub>Si<sub>7</sub>O<sub>9</sub>(OSiMe<sub>3</sub>)(OTl)<sub>2</sub>,<sup>15</sup> was also attempted but did not afford a uniform product either.



The single SiMe<sub>3</sub> resonance in the <sup>1</sup>H, <sup>13</sup>C, and <sup>29</sup>Si NMR spectra of **3** and **4** is consistent with a tetrahedral metal center containing C<sub>2</sub> symmetry. In analogy with its cyclohexyl-substituted analogue, [(*c*-C<sub>6</sub>H<sub>11</sub>)<sub>7</sub>Si<sub>7</sub>O<sub>11</sub>-(OSiMe<sub>3</sub>)<sub>2</sub>Ti],<sup>13</sup> the <sup>13</sup>C and <sup>29</sup>Si NMR spectra of **3** show seven equi-intense resonances (assigned to methine-CH and silsesquioxane framework-Si, respectively), which indicates that the local mirror symmetry of the silsesquioxane ligands is lost.<sup>16</sup> The larger ionic radius of zirconium, compared to titanium, finds expression in a more fluxional complex **4**, as is demonstrated by the coalescence of two pairs of methine-CH and framework-Si resonances in the room-temperature <sup>13</sup>C and <sup>29</sup>Si NMR spectra of **4**, respectively. With five methine-CH resonances (1:2:2:1:1 ratio) and a single Si(CH<sub>3</sub>)<sub>3</sub> signal, the <sup>13</sup>C NMR spectra of **5** and **6** are very similar and in agreement with a C<sub>2</sub> symmetric structure in which the mirror symmetry of the silsesquioxane ligands is retained. The room-temperature <sup>29</sup>Si NMR spectrum of **5** displays six framework-Si resonances (1:1:1:2:1:1 ratio), of which two coalesce at 37 °C (Δ*G*<sup>‡</sup><sub>Tc</sub> = 63.5 kJ/mol)<sup>17</sup> to give the expected set of five signals in a 1:1:1:2:2 ratio.

**X-ray Structure Determination of [(*c*-C<sub>5</sub>H<sub>9</sub>)<sub>7</sub>Si<sub>7</sub>O<sub>11</sub>-(OSiMe<sub>3</sub>)<sub>2</sub>Zr·2THF (**5**).** Crystallization from hexane at -30 °C afforded colorless block-shaped crystals of **5** suitable for an X-ray diffraction study. A perspective view of the molecular structure is shown in Figure 1. Crystal data are collected in Table 2. As for many crystallographically characterized silsesquioxane compounds,<sup>8,15,18</sup> conformational disorder of the cyclopentyl

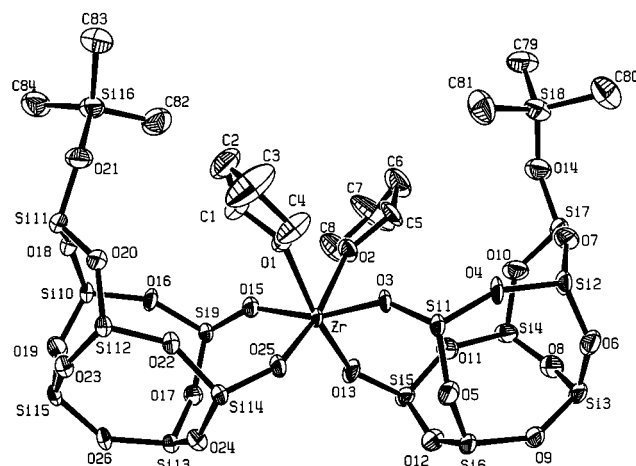


**Figure 1.** Ortep view of [(*c*-C<sub>5</sub>H<sub>9</sub>)<sub>7</sub>Si<sub>7</sub>(OSiMe<sub>3</sub>)O<sub>11</sub>]<sub>2</sub>Zr·2THF (**5**). Ellipsoids are scaled to enclose 30% of the electron density. Hydrogens and cyclopentyl groups are omitted for clarity. Selected bond distances (Å): Zr-O(1), 2.289(5); Zr-O(2), 2.287(5); Zr-O(3), 2.037(4); Zr-O(13), 1.969(4); Zr-O(15), 2.038(5); Zr-O(25), 1.957(4); Si(9)-O(15), 1.590(5); Si(8)-O(14), 1.649(6). Bond angles (deg): O(1)-Zr-O(15), 84.33(17); O(1)-Zr-O(13), 169.60(17); O(2)-Zr-O(13), 89.88(17); O(2)-Zr-O(25), 167.85(18); O(3)-Zr-O(25), 95.37(18); O(3)-Zr-O(15), 161.57(19); Si(7)-O(14)-Si(8), 138.9(4); Si(1)-O(4)-Si(2), 156.3(3).

substituents hampered the refinement. Nevertheless, all relevant atoms could reliably be localized, providing sufficient information concerning the structure.

The six-coordinated zirconium atom in **5** displays a distorted octahedral geometry with *pseudo*-C<sub>2v</sub> symmetry formed by the coordination of two silsesquioxane ligands and two THF molecules. The THF molecules are positioned *cis* to each other. With an average distance of 2.288(5) Å the Zr←O dative bonds in **5** are between the Zr←O bond lengths observed for cationic zirconocene THF adducts and neutral zirconium complexes (ranging from 2.122(14) Å to 2.662(3) Å).<sup>19</sup> An indication that the metal center in this zirconasilsesquioxane complex is quite electrophilic is given by the fact that the THF oxygen atoms in **5** are virtually planar (sum of angles: O(1), 358.0(5)°; O(2), 358.6(5)°), which reflects a rehybridization of the two oxygen donor orbitals to produce an sp<sup>2</sup> type σ-donor orbital and a π-donor orbital of predominantly p character.<sup>19a,b</sup> To optimize the orbital overlap associated with this additional π-interaction, both THF molecules in **5** are orientated nearly perpendicular (O(15)-Zr-O(1)-C(1) = -8.1(5)°; O(3)-Zr-O(2)-C(5) = -9.6(5)°) to the plane formed by O(1), O(2), O(13), and O(25). The Zr-O(3) (2.037(4) Å) and Zr-O(15) (2.038(5) Å) bond lengths are considerably longer than the Zr-O(13) (1.969(4) Å) and Zr-O(25) (1.957(4) Å) bond distances opposite the coordinated THF molecules and the Zr-O bonds in [(*c*-C<sub>6</sub>H<sub>11</sub>)<sub>7</sub>Si<sub>7</sub>O<sub>12</sub>]ZrCp\* (1.958(32) Å).<sup>18a</sup> The Si-O distances (ranging from

(13) Crocker, M.; Herold, R. H. M.; Orpen, A. G. *Chem. Commun.* **1997**, 2411.

(14) Shannon, R. D. *Acta Crystallogr.* **1976**, A32, 751.

(15) Feher, F. J.; Rahimian, K.; Budzichowski, T. A.; Ziller, J. *Organometallics* **1995**, 14, 3920.

(16) This is in agreement with the solid-state structure of **3**, which will be described elsewhere. Vorstenbosch, M. L. W.; Abbenhuis, H. C. L.; van Santen, R. A.; Spek, A. L. To be published.

(17) *T* = 310 K, Δ*ν* = 56.2 Hz, Δ*G*<sup>‡</sup><sub>Tc</sub> = -*RT*<sub>c</sub> ln(πΔ*ν*h/√2*k*<sub>B</sub>*T*<sub>c</sub>); Kessler, H. *Angew. Chem.* **1970**, 82, 237.

(18) For example see: (a) Feher, F. J. *J. Am. Chem. Soc.* **1986**, 108, 3850. (b) Feher, F. J.; Budzichowski, T. A.; Ziller, J. W. *Inorg. Chem.* **1992**, 31, 5100. (c) Buys, I. E.; Hambley, T. W.; Houlton, D. J.; Maschmeyer, T.; Masters, A. F.; Smith, A. K. *J. Mol. Catal.* **1994**, 86, 309.

(19) (a) Jordan, R. F.; Bajgur, C. S.; Willett, R.; Scott, B. *J. Am. Chem. Soc.* **1986**, 108, 7410. (b) Amorose, D. M.; Lee, R. A.; Petersen, J. L. *Organometallics* **1991**, 10, 2191. (c) Giannini, L.; Caselli, A.; Solari, E.; Floriani, C.; Chiesi-Villa, A.; Rizzolli, C.; Re, N.; Sgamellotti, A. *J. Am. Chem. Soc.* **1997**, 119, 9198.

**Table 1. Summary of Ethylene Polymerization Experiments**

catalyst ( $\mu\text{mol}$ )	cocatalyst (mmol)	conditions [min]/[ $^{\circ}\text{C}$ ]/[atm]	PE yield (g)	activity (g/(mmol·h))	$M_w$ ( $\times 10^3$ )	$M_w/M_n$
<b>7</b> (30)		30/25→50/5	0			
<b>7</b> (30)	BF <sub>15</sub> <sup>a</sup> (1)	30/25→50/5	0			
<b>8</b> (30)		7/25/3	0.6	10		
<b>8</b> (20)	BF <sub>15</sub> (1)	7/80/5	5.5	2400	6.6	2.3
<b>8</b> (20)	BF <sub>20</sub> <sup>b</sup> (5.6)	7/80/5	trace	~0		
<b>8</b> (10)	Silica <sup>c</sup> /MAO	7/29/5	9.7	8300 <sup>d</sup>	65	11.7
<b>8</b> (40)	MCM <sup>e</sup> /MAO	7/22→82/5 <sup>f</sup>	12.0	2600 <sup>d</sup>	32	6.8
<b>9</b> (30)		15/25/3	0.5	<10		
<b>9</b> (20)	BF <sub>15</sub> (1)	7/80/5	11.1	4800	82	3.2

<sup>a</sup> BF<sub>15</sub> = B(C<sub>6</sub>F<sub>5</sub>)<sub>3</sub>. <sup>b</sup> BF<sub>20</sub> = [Ph<sub>3</sub>C][B(C<sub>6</sub>F<sub>5</sub>)<sub>4</sub>]. <sup>c</sup> Silica = PQ3040. <sup>d</sup> Assuming that all the catalyst is active. <sup>e</sup> MCM = all-silica MCM-41. <sup>f</sup> Strong temperature increase observed.

**Table 2. Details of the X-ray Structure Determination of [(*c*-C<sub>5</sub>H<sub>9</sub>)<sub>7</sub>Si<sub>7</sub>O<sub>11</sub>(OSiMe<sub>3</sub>)<sub>2</sub>Zr·2THF (**5**) and {[(*c*-C<sub>5</sub>H<sub>9</sub>)<sub>7</sub>Si<sub>7</sub>O<sub>12</sub>]ZrCH<sub>2</sub>Ph}<sub>2</sub> (**8**)**

	<b>5</b>	<b>8</b>
formula	C <sub>84</sub> H <sub>160</sub> O <sub>26</sub> Si <sub>16</sub> Zr·(C <sub>4</sub> H <sub>8</sub> O) <sub>0.72</sub>	(C <sub>42</sub> H <sub>70</sub> O <sub>12</sub> Si <sub>7</sub> Zr) <sub>2</sub>
fw	2178.69	2109.67
cryst system	monoclinic	triclinic
space group, no.	<i>P</i> 2 <sub>1</sub> / <i>c</i> , 14	<i>P</i> 1
<i>a</i> , Å	20.197(3)	13.971(1)
<i>b</i> , Å	15.937(1)	16.172(1)
<i>c</i> , Å	35.006(3)	27.004(2)
$\alpha$ , deg		94.439(6)
$\beta$ , deg	97.02(1)	99.491(7)
$\gamma$ , deg		99.810(7)
<i>V</i> , Å <sup>3</sup>	11 183(2)	5894.7(7)
<i>D</i> <sub>calc</sub> , g cm <sup>-3</sup>	1.294	1.189
<i>Z</i>	4	2
<i>F</i> (000), electrons	4660	2224
$\mu$ (Mo, K $\alpha$ ), cm <sup>-1</sup>	3.4	3.78
cryst size, mm	0.30 $\times$ 0.45 $\times$ 0.50	0.35 $\times$ 0.38 $\times$ 0.50
<i>T</i> , K	130	130
$\theta$ range, deg: min, max	1.01, 24.0	1.24, 25.0
$\lambda$ (Mo, K $\alpha$ ), Å	0.710 73	0.710 73
monochromator	graphite	graphite
$\omega/2\theta$ scan, deg	$\Delta\omega = 0.85 + 0.34 \tan \theta$	$\Delta\omega = 0.90 + 0.34 \tan \theta$
index ranges	<i>h</i> : 0→23; <i>k</i> : 0→18; <i>l</i> : -39→39	<i>h</i> : -16→16; <i>k</i> : 0→19; <i>l</i> : -32→31
total no. of data	18 841	21 882
no. of unique data	17 499	20 604
no. of data with criterion: ( $F_o \geq 4.0\sigma(F_o)$ )	11 440	16 611
$R_{\text{int}} = \sum[ (F_o^2 - F_o^2(\text{mean})) ]/\sum[F_o^2]$		0.038
$R_{\text{sig}} = \sum\sigma(F_o^2)/\sum[F_o^2]$	0.058	0.066
no. of reflections ( $F_o^2 \geq 0$ )	17 481	20 604
no. of refined params	1150	1117
final agreement factors: $wR(F^2) = [\sum[w(F_o^2 - F_c^2)^2]/\sum[w(F_o^2)^2]]^{1/2}$ for $F_o^2 > 0$	0.2090	0.2568
weighting scheme: <i>a</i> , <i>b</i> $w = 1/[\sigma^2(F_o^2) + (aP)^2 + bP]$ and $P = [\max(F_o^2, 0) + 2F_c^2]/3$	0.0633, 87.60	0.1269, 28.00
$R(F) = \sum[ F_o  -  F_c ]/\sum F_o $ for $F_o > 4.0\sigma(F_o)$	0.0818	0.0866
$\text{GoF} = S = [\sum[w(F_o^2 - F_c^2)^2]/(n/p)]^{1/2}$	1.036	1.125
<i>n</i> = no. of refls		
<i>p</i> = no. of params refined residual electron density in final difference Fourier map, e/Å <sup>3</sup>	-1.0, 1.2(1)	-0.88, 2.17(15)
max. (shift/ $\sigma$ ) final cycle	<0.001	<0.001

1.590(5) Å to 1.649(6) Å) and Si–O–Si angles (ranging from 138.9(4)° to 156.3(3)°) in **5** are similar to those observed in other crystallographically characterized (metalla)silsesquioxane compounds.<sup>8,18a</sup>

**Trisilanol III.** Compared to the reactions with **I** and **II**, protolysis of the trisilanol **III** with equimolar amounts of the homoleptic group 4 metal benzyl complexes, M(CH<sub>2</sub>Ph)<sub>4</sub> (M = Ti, Zr, Hf), proceeds surprisingly selectively, affording metallasilsesquioxanes with the general formula [(*c*-C<sub>5</sub>H<sub>9</sub>)<sub>7</sub>Si<sub>7</sub>O<sub>12</sub>]MCH<sub>2</sub>Ph (M = Ti (**7**),<sup>13</sup> Zr (**8**), Hf (**9**), eq 6). In analogy with its cyclohexyl-substituted analogue,<sup>13</sup> both the <sup>13</sup>C and <sup>29</sup>Si NMR spectra of **7** show three resonances in a 3:1:3 ratio, consistent with a monomeric C<sub>3v</sub> corner-capped metallasilsesquioxane complex.<sup>13,18a</sup> To reduce their electron

deficiency, the (formally 8-electron) zirconium and hafnium benzyl complexes (**8**, **9**) form dimeric structures which display much more complicated <sup>1</sup>H, <sup>13</sup>C, and <sup>29</sup>Si spectra (Figure 2, vide infra).

To investigate the fluxional behavior of these dimers in more detail, a variable-temperature <sup>29</sup>Si NMR experiment on toluene solutions of **8** was carried out. In the low-temperature limit (−60 °C), seven equi-intense resonances indicate that all silicon atoms of each metallasilsesquioxane moiety are different. This is in accordance with the solid-state structure of **8** (Figure 2). Upon raising the temperature (from −60 °C to −15 °C), the fluxionality of the metallasilsesquioxane moieties around the siloxy bridges increases, giving five resonances (2:1:1:1:2 ratio) that are in agreement with

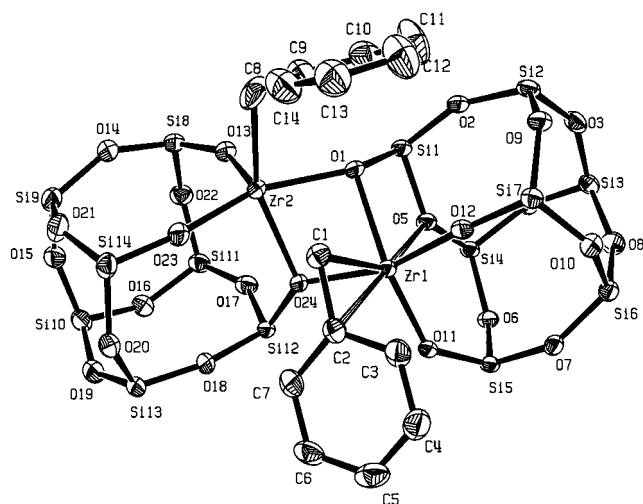
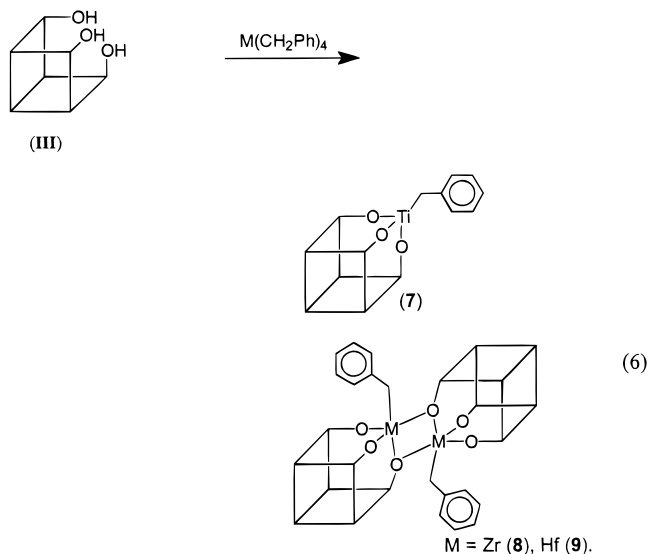


**Figure 2.** ORTEP drawing of  $\{[(c\text{-C}_5\text{H}_9)_7\text{Si}_7\text{O}_{12}]\text{ZrCH}_2\text{Ph}\}_2$  (**8**). Ellipsoids are scaled to enclose 30% of the electron density. Hydrogens and cyclopentyl groups are omitted for clarity. Selected bond distances (Å): Zr(1)–O(1), 2.202(4); Zr(1)–O(5), 2.458(5); Zr(1)–O(11), 1.981(4); Zr(1)–O(12), 1.952(5); Zr(1)–O(24), 2.164(4); Zr(2)–O(1), 2.166(5); Zr(2)–O(13), 1.943(5); Zr(2)–O(23), 1.954(5); Zr(2)–O(24), 2.263(4); Zr(2)–C(8), 2.281(10); Zr(1)–C(1), 2.374(7); Zr(1)–C(2), 2.584(7); Si(1)–O(5), 1.682(5); Si(4)–O(5), 1.674(5); Si(1)–O(2), 1.608(5); Si(5)–O(6), 1.633(5). Bond angles (deg): C(8)–Zr(2)–O(24), 153.6(3); O(1)–Zr(2)–O(23), 159.32(17); O(13)–Zr(2)–C(8), 98.1(3); O(13)–Zr(2)–O(24), 102.65(19); O(13)–Zr(2)–O(23), 99.5(2); O(13)–Zr(2)–O(1), 98.69(18); O(5)–Zr(1)–C(1), 147.6(2); O(5)–Zr(1)–C(2), 175.11(19); O(12)–Zr(1)–O(24), 164.05(17); O(1)–Zr(1)–O(11), 145.02(18); Zr(2)–C(8)–C(9), 124.5(8); Zr(1)–C(1)–C(2), 80.9(4); Si(1)–O(5)–Si(4), 134.0; Si(12)–O(18)–Si(13), 167.3(3).

local mirror symmetry of the silsesquioxane ligands. Further increase of the temperature (from  $-15^\circ\text{C}$  to  $60^\circ\text{C}$ ) eventually yields three resonances with relative intensities of 3:1:3, indicating that at elevated temperature the dimeric structure becomes very fluxional or may even dissociate.



The observation that, unlike **8** and **9**, the titanasil-sesquioxane **7** (formally an 8-electron species) is a monomer in solution is rather surprising. No strong evidence ( $^{13}\text{C}$  NMR, *ipso*- $\text{C}_6\text{H}_5 = 128$  ppm;  $\text{CH}_2\text{Ph}$ ,  $^1J_{\text{C-H}}$

$= 131$  Hz)<sup>20</sup> of  $\eta^n$ -bonding of the benzyl group in **7** could be detected either. Furthermore, like  $[(c\text{-C}_5\text{H}_9)_7\text{Si}_7\text{O}_{11}(\text{OSiMe}_3)]_2\text{Ti}$  (**3**), the titanasil-sesquioxane benzyl complex  $[(c\text{-C}_5\text{H}_9)_7\text{Si}_7\text{O}_{12}]\text{TiCH}_2\text{Ph}$  (**7**) does react with Lewis bases and is recovered unchanged after treatment with THF or acetonitrile. In contrast, **4** and **8**, the zirconium analogues of **3** and **7**, readily form the bis(THF) adducts  $[(c\text{-C}_5\text{H}_9)_7\text{Si}_7\text{O}_{11}(\text{OSiMe}_3)]_2\text{Zr}\cdot 2\text{THF}$  (**5**) and  $[(c\text{-C}_5\text{H}_9)_7\text{Si}_7\text{O}_{12}]\text{ZrCH}_2\text{Ph}\cdot 2\text{THF}$  (**10**) when treated with or synthesized in THF. The difference in ionic radii<sup>14</sup> of titanium and zirconium alone cannot explain that titanium complexes (**3**, **7**) refuse to react with THF whereas the corresponding zirconium compounds (**4**, **8**) react with even 2 equiv of THF. Therefore, the low affinity of **3** and **7** toward Lewis bases is probably electronic in origin. However, why titanasil-sesquioxanes are electronically less unsaturated than the corresponding zirconium complexes is not clear. Titanasil-sesquioxanes and zirconasil-sesquioxane complexes also behave differently with respect to hydrolysis. The  $\equiv\text{SiO-Ti}$  bonds in **3** and **7** are stable toward hydrolysis, whereas the corresponding zirconium compounds (**4**, **8**) hydrolyze rapidly to form the corresponding silanols **II** and **III**, suggesting that the titanium complexes are less ionic than their zirconium analogues.<sup>21</sup>

**X-ray Structure Determination of  $\{[(c\text{-C}_5\text{H}_9)_7\text{Si}_7\text{O}_{12}]\text{ZrCH}_2\text{Ph}\}_2$  (**8**).** Slow crystallization from a cooled ( $-30^\circ\text{C}$ ) saturated hexane solution resulted in pale yellow single crystals of **8** suitable for an X-ray diffraction study. A perspective view of the molecular structure of **8** is shown in Figure 2. Crystal data are collected in Table 2. As observed for **5**, the structure of **8** showed considerable conformational disorder of the silsesquioxane cyclopentyl substituents. Yet, this did not affect the localization of the most relevant atoms. From Figure 2 it is clear that **8** consists of an asymmetric dimeric structure. The dimer is formed by two corner-capped zirconasil-sesquioxane moieties connected by two bridging siloxy functionalities. Typical for electron-deficient dimeric metallasil-sesquioxane complexes, O(1) and O(24) in **8** are  $\mu^2$ -bridged to increase the metal's coordination number. Examples of similar metallasil-sesquioxane complexes containing  $\mu^2$ -bridged siloxy groups are  $\{[\text{R}_7\text{Si}_7\text{O}_{12}]\text{M}\}_2$  ( $\text{M} = \text{Ti}, \text{V}, \text{Al}, \text{Y}$ ;  $\text{R} = c\text{-C}_5\text{H}_9, c\text{-C}_6\text{H}_{11}$ ).<sup>22</sup> Even for less electron-deficient metals dimeric structures are sometimes preferred. In these systems,  $\{[(c\text{-C}_6\text{H}_{11})_7\text{Si}_7\text{O}_{12}]\text{M}\}_2$  ( $\text{M} = \text{B}, \text{TiCp}, \text{V}=\text{O}, \text{Mo}$ ),<sup>18b,c,23</sup> the dimeric structure is maintained by siloxy functionalities that are  $\sigma$ -bonded to the adjacent metal center. Although entropically unfavorable, these dimers are formed to optimize  $\text{O}(\text{p}\pi)\text{-M}(\text{d}\pi)$  bonding, which is less effective in monomeric structures for which the Si–O–M angles

(20)  $\eta^n$ -bonding of a benzyl group is accompanied with a highfield shift of the *ipso*-carbon of the benzyl group, and a large  $^1J_{\text{C-H}}$  ( $> 140$  Hz) for the benzylic  $\text{CH}_2$  group. For example see: (a) Jordan, R. F.; LaPointe, R. E.; Bajgur, C. S.; Echols, S. F.; Willet, R. *J. Am. Chem. Soc.* **1987**, *109*, 4111. (b) Jordan, R. F.; LaPointe, R. E.; Baenziger, N. C.; Hinch, G. D. *Organometallics* **1990**, *9*, 1539. (c) Bochmann, M.; Lancaster, S. J. *Organometallics* **1993**, *12*, 633. (d) Bochmann, M.; Lancaster, S. J.; Hursthouse, M. B.; Malik, K. M. A. *Organometallics* **1994**, *13*, 2235.

(21) The stability toward hydrolysis of the titanium–siloxy bonds in **3** and **7** is in agreement with that of TS-1 and Ti-Beta, which are effective oxidation catalysts in an aqueous environment. For example see: Corma, A.; Esteve, P.; Matínez, A.; Valencia, S. *J. Catal.* **1995**, *152*, 18, and references therein.



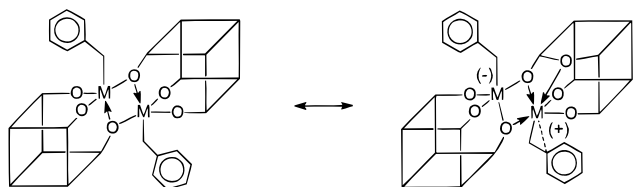
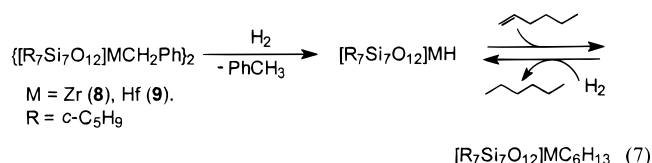


**Figure 3.** Proposed resonance structures for  $\{[(\text{C-C}_5\text{H}_9)_7\text{Si}_7\text{O}_{12}]\text{ZrCH}_2\text{Ph}\}_2$  (**8**).

are more acute.<sup>22c</sup> Accordingly, O(1) is more strongly bonded to Zr(2) (2.166(5) Å) than to Zr(1) (2.202(4) Å), whereas O(24) is more strongly bonded to Zr(1) (2.164(4) Å) than to Zr(2) (2.263(4) Å). As expected, the  $\mu^2$ -bridged oxygens in **8** form weaker bonds with the zirconium than the nonbridging oxygens (1.943(5)–1.981(4) Å), for which the distances are comparable to the Zr–O  $\sigma$ -bonds in, for example, **5**,  $[(\text{C-C}_6\text{H}_{11}\text{O}_7\text{Si}_7\text{O}_{12})\text{ZrCp}^*]_2$ ,<sup>18a</sup> and  $[2,6-(\text{Me}_3\text{C})_2\text{C}_6\text{H}_3]\text{OZr}(\text{CH}_2\text{Ph})_3$ .<sup>10b</sup> The coordination environment of Zr(2) can best be described as distorted square-pyramidal with O(13) occupying the axial position ( $\text{C}(8)\text{--Zr}(2)\text{--O}(24) = 153.6(3)^\circ$ ,  $\text{O}(1)\text{--Zr}(2)\text{--O}(23) = 159.32(17)^\circ$ ,  $\text{O}(13)\text{--Zr}(2)\text{--C}(8) = 98.1(3)^\circ$ ,  $\text{O}(13)\text{--Zr}(2)\text{--O}(24) = 102.65(19)^\circ$ ,  $\text{O}(13)\text{--Zr}(2)\text{--O}(23) = 99.5(2)^\circ$ ,  $\text{O}(13)\text{--Zr}(2)\text{--O}(1) = 98.69(18)^\circ$ ). The coordination environment of Zr(1) is more complex due to the additional coordination of O(5) and C(2) to the metal center. Considering the benzyl C(1) and C(2) atoms to occupy one coordination vertex, the zirconium environment can best be described as distorted octahedral ( $\text{O}(5)\text{--Zr}(1)\text{--C}(1) = 147.6(2)^\circ$ ,  $\text{O}(5)\text{--Zr}(1)\text{--C}(2) = 175.11(19)^\circ$ ,  $\text{O}(12)\text{--Zr}(1)\text{--O}(24) = 164.05(17)^\circ$ ,  $\text{O}(1)\text{--Zr}(1)\text{--O}(11) = 145.02(18)^\circ$ ). Whereas for Zr(2) the benzyl group is bonded in a normal  $\eta^1$  fashion ( $\text{Zr}(2)\text{--C}(8) = 2.281(10)$  Å,  $\text{Zr}(2)\text{--C}(8)\text{--C}(9) = 124.5(8)^\circ$ , the acute  $\text{Zr}(1)\text{--C}(1)\text{--C}(2)$  angle ( $80.9(4)^\circ$ ) and the short  $\text{Zr}(1)\text{--C}(2)$  distance (2.584(7) Å) are characteristic for an  $\eta^2$ -bonded benzyl group.<sup>20,24</sup> Besides the  $\eta^2$ -bonding mode of the benzyl group, Zr(1) gains additional electron density by coordination of O(5). With a distance of 2.458(5) Å, the  $\text{Zr}(1)\leftarrow\text{O}(5)$  dative bond is normal within the range found for other zirconium complexes.<sup>19</sup> A similar intramolecular interaction of a silyl ether was observed in a dimeric yttrium silsesquioxane complex.<sup>22d</sup> Coordination of silyl ether functionalities to Lewis acidic metal centers has also been proposed to occur in corresponding oxide-supported systems.<sup>6c,25</sup> The additional coordination of O(5) and the  $\eta^2$ -bonding of the benzyl group suggest that Zr(1) is more electron-deficient than Zr(2). A possible explanation for this phenomenon is given by the zwitterionic resonance structure as proposed in Figure 3. Although the comparable Zr(1)–O and Zr(2)–O distances in the system

do not strongly support such a structure, it is clear that Zr(1) shows all the characteristics of a strong electron-deficient metal center, similar to that in cationic zirconium systems. In contrast, Zr(2) does not show any signs of being very electron-deficient. Due to the coordination of O(5) to Zr(1), the Si(1)–O(5) (1.682(5) Å) and Si(4)–O(5) (1.674(5) Å) bonds are significantly longer than the other Si–O bonds (1.608(5)–1.633(5) Å) that form the silsesquioxane framework. Although the silsesquioxane Si–O–Si span a wide range of angles (from  $134.0(3)^\circ$  to  $167.3(3)^\circ$ ), they are not exceptional.<sup>8,18,22,23</sup>

**M–C  $\sigma$ -Bond Hydrogenolysis.** Both the monomeric (**7**) and dimeric (**8**, **9**) silsesquioxane benzyl complexes are interesting models for Basset's silica-grafted group 4 metal carbonyl and hydride systems.<sup>6d,e,26</sup> Grafting of  $\text{MR}_4$  onto partly dehydroxylated silica affords species of the type  $[\equiv\text{SiO}]\text{MR}_3$ . Subsequent hydrogenolysis of these immobilized tris(carbonyl) complexes has been found to yield mono(hydride) systems  $[\equiv\text{SiO}]\text{MH}$  ( $\text{M} = \text{Ti}, \text{Zr}, \text{Hf}$ ), whose general structure is similar to that of **7**–**9**.<sup>6d,e,26</sup> As a first test to determine the suitability of metallasilsesquioxane complexes as models for silica-grafted species, M–C  $\sigma$ -bond hydrogenolysis of **7**–**9** to form the corresponding metallasilsesquioxane hydrides, “ $[(\text{C-C}_5\text{H}_9)_7\text{Si}_7\text{O}_{12}]\text{MH}$ ”, was attempted. Exposure of the zirconium and hafnium silsesquioxane benzyl complexes **8** and **9** to dihydrogen (toluene, 50 °C, 3 atm  $\text{H}_2$ ) resulted in the slow (10–20 h) hydrogenolysis of the M–C bond with concomitant quantitative formation of toluene. Poor crystallinity, complex NMR spectra, and insufficient thermal stability frustrated the isolation and characterization of the zirconium and hafnium hydrides. Nevertheless, the existence of these hydrides could be proven by the catalytic hydrogenation of 1-hexene to *n*-hexane (eq 7). The monomeric titanasilsesquioxane benzyl complex **7** is much less susceptible to Ti–C bond hydrogenolysis: after 48 h at 75 °C under 4 atm of  $\text{H}_2$  and in the presence of 1-hexene, both the benzyl complex and the 1-hexene were recovered unchanged. Likewise, the coordinatively saturated bis(THF) adduct **10** did not react with dihydrogen under the conditions that proved to be sufficient to hydrogenolyze **8** and **9**.



**Olefin Polymerization.** Oxide-supported zirconium hydride and alkyl species are known to effectively insert C=C double bonds. Recently, Basset et al. reported the synthesis of a aluminosilicate-supported zirconium hydride.<sup>26b</sup> The authors argued that introduction of electrophilic aluminum centers on the support enhances the olefin polymerization activity of the catalyst compared to the all-silica system. That Lewis acidic aluminum sites on oxide supports can positively influence the catalyst's activity was also demonstrated by, for example, Colette<sup>2b,g</sup> and Moroz,<sup>27</sup> who found that alumina-

(22) (a) Feher, F. J.; Gonzales, S. L.; Ziller, J. W. *Inorg. Chem.* **1988**, *27*, 3440. (b) Feher, F. J.; Walzer, J. F. *Inorg. Chem.* **1990**, *29*, 1604. (c) Feher, F. J.; Budzichowski, T. A.; Weller, K. J. *J. Am. Chem. Soc.* **1989**, *111*, 7288. (d) Herrmann, W. A.; Anwender, R.; Dufaud, V.; Scherer, W. *Angew. Chem.* **1994**, *106*, 1338.

(23) (a) Feher, F. J.; Walzer, J. F. *Inorg. Chem.* **1991**, *30*, 1689. (b) Budzichowski, T. A.; Chacon, S. T.; Chisholm, M. H.; Feher, F. J.; Streib, W. *J. Am. Chem. Soc.* **1991**, *113*, 689.

(24) (a) Hughes, A. K.; Meetsma, A.; Teuben, J. H. *Organometallics* **1993**, *12*, 1936. (b) Davies, G. R.; Jarvis, J. A. *J. Chem. Soc., Chem. Commun.* **1971**, 1511. (c) Latsky, S. L.; McMullen, A. K.; Niccolai, G. P.; Rothwell, I. P.; Huffman, J. C. *Organometallics* **1985**, *4*, 902. (d) Latsky, S. L.; McMullen, A. K.; Niccolai, G. P.; Rothwell, I. P.; Huffman, J. C. *Organometallics* **1985**, *4*, 902. (e) Mintz, E. A.; Moloy, K. G.; Marks, T. J. *J. Am. Chem. Soc.* **1982**, *104*, 4692.

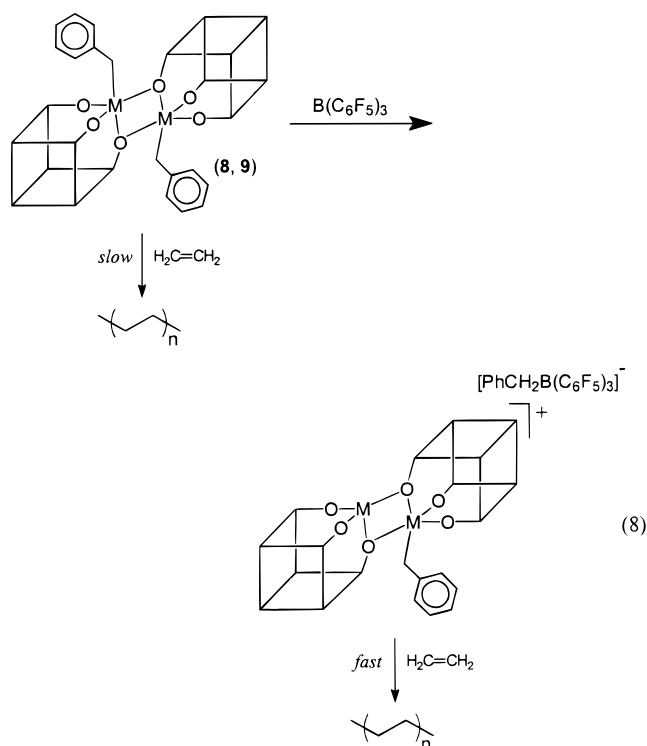
(25) Liebau, F. *Structural Chemistry of Silicates*; Springer: Berlin, 1985.

(26) (a) Rosier, C.; Niccolai, G. P.; Basset, J.-M. *J. Am. Chem. Soc.* **1997**, *119*, 12408. (b) Dufaud, V.; Basset, J.-M. *Angew. Chem.* **1998**, *110*, 848. (c) d'Ornelas, L.; Reyes, S.; Quignard, F.; Choplin, A.; Basset, J.-M. *Chem. Lett.* **1993**, 1931.

or aluminosilicate-supported zirconium alkyl complexes are active ethylene polymerization catalysts (without cocatalysts), whereas the unsupported zirconium alkyls are inactive.

The silsesquioxane-stabilized benzyl complexes **7–9** are probably the most realistic model systems for silica-supported group 4 metal carbyl or hydride species known to date. In the dimeric structure of **8**, the electron density appears to be unevenly divided between the metal centers (Figures 2, 3). One could argue that Zr(2) acts as an internal cocatalyst (comparable to acidic aluminum sites on oxide supports), withdrawing electron density from Zr(1).<sup>2a,b,26b,27</sup> Such an intramolecular activation would render the use of a cocatalyst superfluous.

Preliminary ethylene polymerization experiments in which **7–9** were used without the addition of a cocatalyst revealed that the dimeric metallasilsesquioxane benzyl complexes **8** and **9** are indeed active ethylene polymerization catalysts (eq 8), whereas the monomeric titanasilsesquioxane **7** is inactive. Although the activity of **8** and **9** in ethylene polymerization is low (Table 1), the polarization in the dimeric structures (**8**, **9**) is sufficiently strong to activate the system at least to some extent. This activating synergism between the two metal centers is expected to intensify when one of the two benzyl groups is removed by a cocatalyst, forming a dimeric mono(benzyl) cation. In the presence of  $B(C_6F_5)_3$  the ethylene polymerization activity of both **8** and **9** does indeed increase considerably (Table 1, eq 8). Hence, introducing a positive charge on one of the metal centers results in activation of the adjacent metal alkyl bond.



<sup>1</sup>H, <sup>11</sup>B, and <sup>19</sup>F NMR studies on  $B(C_6F_5)_3$  containing solutions of **8** and **9** showed that even with an excess

(10 equiv) of cocatalyst present, these systems react exclusively with 1 equiv of  $B(C_6F_5)_3$ , yielding the expected cationic mono(benzyl) complexes,  $\{[(C-C_5H_9)_7Si_7O_{12}]_2M_2CH_2Ph\}^+$  ( $M = Zr, Hf$ ). In the <sup>19</sup>F NMR spectra, the small  $\Delta\delta(F_m - F_p)$  values for the  $[(C_6F_5)_3-BCH_2Ph]^-$  anion (**8** +  $B(C_6F_5)_3$ ,  $\Delta\delta(F_m - F_p) = 2.59$  ppm; **9** +  $B(C_6F_5)_3$ ,  $\Delta\delta(F_m - F_p) = 2.46$  ppm) indicate that no significant anion–cation interaction is present in these systems.<sup>28</sup> The cationic complexes have a limited thermal stability and gradually decompose at room temperature. When activated with  $[Ph_3C]^+[B(C_6F_5)_4]^-$ , the polymerization activity of both **8** and **9** dropped dramatically compared to the  $B(C_6F_5)_3$ -activated systems. NMR studies showed that whereas  $B(C_6F_5)_3$  reversibly abstracts only one benzyl group per dimer,  $[Ph_3C]^+[B(C_6F_5)_4]^-$  is electrophilic enough to irreversibly remove both benzyl groups, yielding inactive complexes of the type  $\{[(C-C_5H_9)_7Si_7O_{12}]M\}^+\{B(C_6F_5)_4\}^-$ .

The molecular weight of the polyethylene formed with  $B(C_6F_5)_3$ -activated **8** ( $M_w = 6600$ ) is considerably lower than for the corresponding hafnium system (**9**:  $M_w = 82000$ ). With a  $M_w/M_n$  of 2.3 and 3.2, respectively, both the zirconium and hafnium systems can be considered as single-site catalysts. Opposite of what is usually observed, the hafnium complex **9** forms a more active catalyst than the zirconium complex **8** when activated with  $B(C_6F_5)_3$  (Table 1). A plausible explanation for this phenomenon is the fact that the zirconium complex is thermally less stable than its hafnium analogue (qualitatively determined with <sup>1</sup>H NMR), which will result in faster catalyst deactivation of the zirconium complex at higher polymerization temperatures (80 °C, Table 1).

Immobilization of **8** on MAO-pretreated silica (PQ3040) and all-silica MCM-41 also gave active ethylene polymerization catalysts. The resulting heterogeneous catalysts showed an activity comparable to or even higher than observed for the unsupported **8** +  $B(C_6F_5)_3$  system (Table 1). This is quite surprising since heterogenization of homogeneous metallocene catalysts often goes together with loss of activity.<sup>2</sup> As expected for a heterogeneous catalyst, the polyethylene prepared with immobilized **8** showed a much better morphology (spherical particles) and gave considerably less reactor fouling than the homogeneously prepared polymer, which was isolated as a gel. Immobilization of **8** resulted in increase in molecular weight by a factor of 10; however, the rather high polydispersity of the polyethylene indicates that it is probably not formed by a single-site catalyst (Table 1). This is not surprising keeping in mind that without cocatalyst **8** is also an active ethylene polymerization catalyst. Furthermore, there is a realistic chance that (partial) substitution of the silsesquioxane ligands takes place since aluminumalkyls (including MAO) are known to be able to split metal siloxy,  $M-OSi\equiv$ , bonds.<sup>29</sup> This could subsequently lead to new catalytically active complexes which contribute to the high polydispersity.

Although being reasonably active single-site ethylene polymerization catalysts (Table 1), the  $B(C_6F_5)_3$ -acti-

(28) (a) Pellecchia, C.; Immirzi, A.; Grassi, A.; Zambelli, A. *Organometallics* **1993**, *12*, 4473. (b) Horton, A. D.; de With, J.; van der Linden, A. J.; van de Weg, H. *Organometallics* **1996**, *15*, 2672.

(29) Reactivity studies of metallasilsesquioxane complexes have shown that aluminum alkyls are able to split  $M-OSi\equiv$  bonds, resulting in leaching of the silsesquioxane ligand: (a) Feher, F. J.; Blanski, R. L. *J. Am. Chem. Soc.* **1992**, *114*, 5886. (b) Reference 9.

(27) Moroz, B. L.; Semikolenova, N. V.; Nosov, A. V.; Zakharov, V. A.; Nagy, S.; O'Reilly, N. J. *J. Mol. Catal.* **1998**, *130*, 121.



vated metallasilsesquioxanes **8** and **9** show no polymerization activity for  $\alpha$ -olefins (propene, 1-hexene) at all. As expected, the monomeric titanasilsesquioxane complex **7** remains inactive upon addition of  $\text{B}(\text{C}_6\text{F}_5)_3$  or  $[\text{Ph}_3\text{C}]^+[\text{B}(\text{C}_6\text{F}_5)_4]^-$ , which suggests that the dimeric structure of metallasilsesquioxanes **8** and **9** plays an important role.

### Concluding Remarks

The results presented here emphasize the earlier proposed suitability of silsesquioxanes to mimic surface silanol sites. Besides being useful soluble model systems that can provide significant information about reactions taking place at silica surfaces, the metallasilsesquioxane complexes **8** and **9** are very interesting catalysts themselves.

One of the shortcomings of homogeneous model systems is clearly demonstrated by the reactions with **I** and **II**: When soluble silsesquioxanes (**I** or **II**) are used instead of solid supports, bimolecular reactions result in the formation of thermodynamically stable complexes such as **3** and **4** or product mixtures.

A peculiar observation is the significantly higher electrophilic character of zirconium compared to titanium. Although formally 8-electron species, titanasilsesquioxanes **3** and **7** refuse to react with strong Lewis bases such as THF or even the sterically unhindered MeCN. In contrast, silsesquioxane-stabilized zirconium and hafnium complexes satisfy their electron deficiency by forming dimeric structures (**8**, **9**) or bis(THF) adducts (**5**, **6**, **10**). The reason for this difference in electrophilicity is not yet understood.

Most intriguing of all is the apparent intramolecular activating ability of the dimeric benzyl complexes **8** and **9**, which, like their heterogeneous congeners,<sup>2b,g,26b</sup> are active ethylene polymerization catalysts even without a cocatalyst. This activating synergism between the two metal centers in **8** and **9** is intensified by the addition of  $\text{B}(\text{C}_6\text{F}_5)_3$ , which increases the catalyst's activity by more than 2 orders of magnitude.

### Experimental Section

**General Comments.** All manipulations were performed under an argon atmosphere using box (Braun MB-150 GI) and Schlenk techniques. Solvents were distilled from Na (toluene), K (THF), Na/K alloy (ether, hexanes), or CaH<sub>2</sub> (CH<sub>2</sub>Cl<sub>2</sub>) and stored under argon. NMR solvents were dried over Na/K alloy (benzene-*d*<sub>6</sub>, toluene-*d*<sub>8</sub>) or 4 Å molecular sieves (CDCl<sub>3</sub>). NMR spectra were recorded on a Varian GEMINI 300 and Bruker AC400 spectrometers. Chemical shifts are reported in ppm and referenced to residual solvent resonances (<sup>1</sup>H, <sup>13</sup>C NMR) or external standards (<sup>11</sup>B, BF<sub>3</sub>·OEt<sub>2</sub> = 0 ppm; <sup>19</sup>F, CF<sub>3</sub>CO<sub>2</sub>H = 0 ppm; <sup>29</sup>Si, SiMe<sub>4</sub> = 0 ppm). Elemental analyses were carried out at the Analytical Department of the University of Groningen (The Netherlands). To reduce the often observed silicon carbide formation, V<sub>2</sub>O<sub>5</sub> was added to improve the combustion. Silsesquioxanes (*c*-C<sub>5</sub>H<sub>9</sub>)<sub>7</sub>Si<sub>8</sub>O<sub>12</sub>(OH) (**I**),<sup>9</sup> (*c*-C<sub>5</sub>H<sub>9</sub>)<sub>7</sub>Si<sub>7</sub>O<sub>9</sub>(OSiMe<sub>3</sub>)(OH)<sub>2</sub> (**II**),<sup>8a</sup> (*c*-C<sub>5</sub>H<sub>9</sub>)<sub>7</sub>Si<sub>7</sub>O<sub>9</sub>(OH)<sub>3</sub> (**III**),<sup>8a</sup> and group 4 metal benzyl complexes M(CH<sub>2</sub>Ph)<sub>4</sub> (M = Ti, Zr, Hf)<sup>30a</sup> and (PhCH<sub>2</sub>)<sub>2</sub>-ZrCl<sub>2</sub>·OEt<sub>2</sub><sup>30b</sup> were prepared following literature procedures. ZrCl<sub>4</sub> (Merck) was sublimed twice before use. HfCl<sub>4</sub> (ACROS) and TiCl<sub>4</sub> (Aldrich) were used without further purifications. Experimental details of Cp''[(*c*-C<sub>5</sub>H<sub>9</sub>)<sub>7</sub>Si<sub>8</sub>O<sub>13</sub>](Ti(CH<sub>2</sub>Ph)<sub>2</sub>) (**1**) are described in detail elsewhere.<sup>9</sup>

**[(*c*-C<sub>5</sub>H<sub>9</sub>)<sub>7</sub>Si<sub>8</sub>O<sub>13</sub>](TiCl<sub>3</sub>) (**2**).** At room temperature, a solution of (*c*-C<sub>5</sub>H<sub>9</sub>)<sub>7</sub>Si<sub>8</sub>O<sub>12</sub>(OH) (**I**: 2.92 g, 3.18 mmol) in hexane (30 mL) was added to a hexane (50 mL) solution of TiCl<sub>4</sub> (1.5 mL, 13.7 mmol). Upon addition, the reaction mixture turned reddish and colorless microcrystalline material precipitated. The volatiles were removed in a vacuum, and the crude product was dissolved in hot toluene (20 mL). Crystallization at room temperature yielded **2** as block-shaped off-white crystals (1.2 g, 1.1 mmol, 35%). Cooling of the mother liquor to -30 °C yielded a second crop of **2** as white microcrystalline material (0.7 g, 0.7 mmol, 21%). <sup>1</sup>H NMR (CDCl<sub>3</sub>,  $\delta$ ): 1.80 (m, 14H, CH<sub>2</sub>-C<sub>5</sub>H<sub>9</sub>), 1.55 (m, 42H, CH<sub>2</sub>-C<sub>5</sub>H<sub>9</sub>), 1.07 (m, 7H, CH-C<sub>5</sub>H<sub>9</sub>). <sup>13</sup>C NMR (CDCl<sub>3</sub>,  $\delta$ ): 27.21 (t, CH<sub>2</sub>-C<sub>5</sub>H<sub>9</sub>, <sup>1</sup>J<sub>C-H</sub> = 129 Hz), 27.16 (t, CH<sub>2</sub>-C<sub>5</sub>H<sub>9</sub>, <sup>1</sup>J<sub>C-H</sub> = 129 Hz), 26.95 (t, CH<sub>2</sub>-C<sub>5</sub>H<sub>9</sub>, <sup>1</sup>J<sub>C-H</sub> = 129 Hz), 22.09 (d, CH-C<sub>5</sub>H<sub>9</sub>, <sup>1</sup>J<sub>C-H</sub> = 119 Hz), 22.00 (d, CH-C<sub>5</sub>H<sub>9</sub>, <sup>1</sup>J<sub>C-H</sub> = 119 Hz), 21.80 (d, CH-C<sub>5</sub>H<sub>9</sub>, <sup>1</sup>J<sub>C-H</sub> = 121 Hz). <sup>29</sup>Si NMR (CH<sub>2</sub>Cl<sub>2</sub>,  $\delta$ ): -65.82, -67.04, -113.48 (3:4:1). Anal. Calcd for C<sub>35</sub>H<sub>63</sub>Cl<sub>3</sub>O<sub>13</sub>Si<sub>8</sub>Ti: C, 39.26; H, 5.93; Ti, 4.47. Found: C, 39.72; H, 6.04; Ti, 4.25.

**[(*c*-C<sub>5</sub>H<sub>9</sub>)<sub>7</sub>Si<sub>7</sub>O<sub>11</sub>(OSiMe<sub>3</sub>)<sub>2</sub>](Ti) (**3**).** At -80 °C, Ti(CH<sub>2</sub>Ph)<sub>4</sub> (0.37 g 0.90 mmol) was added to a solution of (*c*-C<sub>5</sub>H<sub>9</sub>)<sub>7</sub>Si<sub>7</sub>O<sub>9</sub>(OSiMe<sub>3</sub>)(OH)<sub>2</sub> (**II**: 1.6 g, 1.7 mmol) in toluene (30 mL). Upon warming to room temperature, the solution decolorized. After stirring for an additional hour at room temperature, the solvent was evaporated and the product was extracted with hexane (30 mL). Evaporation to dryness and subsequent recrystallization from CH<sub>2</sub>Cl<sub>2</sub> gave **3** as a white microcrystalline material which lost lattice solvent upon drying. Yield: 1.1 g (0.6 mmol, 67%). <sup>1</sup>H NMR (CDCl<sub>3</sub>,  $\delta$ ): 1.80 (m, 14H, CH<sub>2</sub>-C<sub>5</sub>H<sub>9</sub>), 1.62 (m, 42H, CH<sub>2</sub>-C<sub>5</sub>H<sub>9</sub>), 1.01 (m, 7H, CH-C<sub>5</sub>H<sub>9</sub>), 0.21 (s, 9H, Si(CH<sub>3</sub>)<sub>3</sub>). <sup>13</sup>C{<sup>1</sup>H} NMR (CDCl<sub>3</sub>,  $\delta$ ): 27.79, 27.65, 27.53, 27.39, 27.09, 26.99 (s, CH<sub>2</sub>-C<sub>5</sub>H<sub>9</sub>); 24.36, 23.50, 23.21, 23.12, 23.02, 22.47, 22.35 (s, CH-C<sub>5</sub>H<sub>9</sub>); 1.93 (s, Si(CH<sub>3</sub>)<sub>3</sub>). <sup>29</sup>Si NMR (toluene,  $\delta$ ): 9.14 (S/Me<sub>3</sub>), -65.16, -65.70, -66.33, -67.09, -68.02, -68.22, -68.33. Anal. Calcd for C<sub>76</sub>H<sub>144</sub>O<sub>24</sub>Si<sub>16</sub>Ti: C, 47.07; H, 7.48; Ti, 2.47. Found: C, 46.99; H, 7.59; Ti, 2.42.

**[(*c*-C<sub>5</sub>H<sub>9</sub>)<sub>7</sub>Si<sub>7</sub>O<sub>11</sub>(OSiMe<sub>3</sub>)<sub>2</sub>](Zr) (**4**).** To a solution of Zr(CH<sub>2</sub>Ph)<sub>4</sub> (0.40 g, 0.88 mmol) in toluene (20 mL) was added (*c*-C<sub>5</sub>H<sub>9</sub>)<sub>7</sub>Si<sub>7</sub>O<sub>9</sub>(OSiMe<sub>3</sub>)(OH)<sub>2</sub> (**II**: 1.66 g, 1.75 mmol) at -50 °C. Immediately the solution decolorized. The mixture was allowed to warm to room temperature and was stirred for 1 h. The volatiles were removed in a vacuum, and the crude product was extracted with and recrystallized from hot hexane (10 mL). Yield: 1.05 g (0.53 mmol, 60%). <sup>1</sup>H NMR (CDCl<sub>3</sub>,  $\delta$ ): 1.79 (m, 14H, CH<sub>2</sub>-C<sub>5</sub>H<sub>9</sub>), 1.63 (m, 14H, CH<sub>2</sub>-C<sub>5</sub>H<sub>9</sub>), 1.52 (m, 28H, CH<sub>2</sub>-C<sub>5</sub>H<sub>9</sub>), 0.98 (m, 7H, CH-C<sub>5</sub>H<sub>9</sub>), 0.23 (s, 9H, Si(CH<sub>3</sub>)<sub>3</sub>). <sup>13</sup>C{<sup>1</sup>H} NMR (CDCl<sub>3</sub>,  $\delta$ ): 27.59, 27.49, 27.40, 27.34, 27.10, 27.04, 26.97 (s, CH<sub>2</sub>-C<sub>5</sub>H<sub>9</sub>); 24.26, 23.52, 23.29, 22.51, 22.42 (s, CH-C<sub>5</sub>H<sub>9</sub>). <sup>13</sup>C NMR (CDCl<sub>3</sub>,  $\delta$ ): 1.88 (q, Si(CH<sub>3</sub>)<sub>3</sub>, <sup>1</sup>J<sub>C-H</sub> = 118 Hz). <sup>29</sup>Si NMR (toluene, 323 K,  $\delta$ ): 9.44 (S/Me<sub>3</sub>), -65.14, -65.55, -65.72, -66.63, -67.77 (1:1:1:1:2:2). Anal. Calcd for C<sub>76</sub>H<sub>144</sub>O<sub>24</sub>Si<sub>16</sub>Zr: C, 46.04; H, 7.32; Zr, 4.60. Found: C, 46.16; H, 7.45; Zr, 4.54.

**[(*c*-C<sub>5</sub>H<sub>9</sub>)<sub>7</sub>Si<sub>7</sub>O<sub>11</sub>(OSiMe<sub>3</sub>)<sub>2</sub>](Zr·2THF) (**5**).** A THF (20 mL) solution of Zr(CH<sub>2</sub>Ph)<sub>4</sub> (0.61 g, 1.34 mmol) was treated with (*c*-C<sub>5</sub>H<sub>9</sub>)<sub>7</sub>Si<sub>7</sub>O<sub>9</sub>(OSiMe<sub>3</sub>)(OH)<sub>2</sub> (**II**: 2.52 g, 2.66 mmol) at -80 °C. The mixture was allowed to warm to room temperature, upon which the color of the solution turned from bright to pale yellow. The solvent was evaporated, and the crude product was dissolved in CH<sub>2</sub>Cl<sub>2</sub> (10 mL) and filtered to remove minor amounts of insoluble impurities. Slow evaporation of the CH<sub>2</sub>Cl<sub>2</sub> at room temperature yielded **5** as large block-shaped crystals (1.64 g, 0.77 mmol, 58%). Since the crystals slowly lost THF incorporated in the lattice, the crystals were powdered and dried thoroughly. <sup>1</sup>H NMR (CDCl<sub>3</sub>,  $\delta$ ): 4.20 (m, 4H, THF- $\alpha$ -CH<sub>2</sub>), 1.96 (m, 4H, THF- $\beta$ -CH<sub>2</sub>), 1.77 (m, 14H, CH<sub>2</sub>-C<sub>5</sub>H<sub>9</sub>), 1.61 (m, 14H, CH<sub>2</sub>-C<sub>5</sub>H<sub>9</sub>), 1.51 (m, 28H, CH<sub>2</sub>-C<sub>5</sub>H<sub>9</sub>), 0.97 (m, 7H, CH-C<sub>5</sub>H<sub>9</sub>), 0.17 (s, 9H, Si(CH<sub>3</sub>)<sub>3</sub>). <sup>13</sup>C{<sup>1</sup>H} NMR (CDCl<sub>3</sub>,  $\delta$ ): 71.19 (s, THF- $\alpha$ -CH<sub>2</sub>), 28.16, 27.85, 27.74, 27.67, 27.60, 27.55, 27.45, 27.13, 26.97, 26.93 (s, CH-C<sub>5</sub>H<sub>9</sub>), 25.30 (s, THF- $\beta$ -CH<sub>2</sub>), 25.00, 24.10, 23.86, 22.67, 22.49 (s, CH-C<sub>5</sub>H<sub>9</sub>),

1:2:2:1:1), 2.00 (s, Si(CH<sub>3</sub>)<sub>3</sub>). <sup>29</sup>Si NMR (THF, 283 K, δ): 8.18 (SiMe<sub>3</sub>), -64.10, -64.79, -65.88, -67.28, -68.40, -69.10 (1:1:1:1:2:1:1). Anal. Calcd for C<sub>84</sub>H<sub>160</sub>O<sub>26</sub>Si<sub>16</sub>Zr: C, 47.44; H, 7.58; Zr, 4.29. Found: C, 46.85; H, 7.45; Zr, 4.36.

**[(c-C<sub>5</sub>H<sub>9</sub>)<sub>7</sub>Si<sub>7</sub>O<sub>11</sub>(OSiMe<sub>3</sub>)<sub>2</sub>]ZrCl<sub>2</sub>·2THF (**6**).** At room temperature, solid (c-C<sub>5</sub>H<sub>9</sub>)<sub>7</sub>Si<sub>7</sub>O<sub>9</sub>(OSiMe<sub>3</sub>)(OH)<sub>2</sub> (**II**, 4.62 g, 4.88 mmol) was added to a stirred THF (50 mL) solution of (PhCH<sub>2</sub>)<sub>2</sub>ZrCl<sub>2</sub>·OEt<sub>2</sub> (2.02 g, 4.83 mmol). Immediately, the yellow solution decolorized. After 5 min, the solvent was evaporated and the product was dried thoroughly. The product was dissolved in dichloromethane (20 mL) and filtered. Concentration and cooling to -30 °C yielded **6** (2.50 g, 2.00 mmol, 41%) as colorless crystals. The mother liquor was evaporated to dryness, and the remaining solid was dissolved in hexane (10 mL). After filtration the clear solution was concentration and cooled to -30 °C, yielding a second crop of **6** as microcrystalline material (1.3 g, 1.04 mmol, 22%). <sup>1</sup>H NMR (CDCl<sub>3</sub>, δ): 4.34 (m, 8H, THF-α-CH<sub>2</sub>), 2.03 (m, 8H, THF-β-CH<sub>2</sub>), 1.77 (m, 14H, CH<sub>2</sub>-C<sub>5</sub>H<sub>9</sub>), 1.61 (m, 14H, CH<sub>2</sub>-C<sub>5</sub>H<sub>9</sub>), 1.51 (m, 28H, CH<sub>2</sub>-C<sub>5</sub>H<sub>9</sub>), 0.97 (m, 7H, CH-C<sub>5</sub>H<sub>9</sub>), 0.10 (s, 9H, Si(CH<sub>3</sub>)<sub>3</sub>). <sup>13</sup>C{<sup>1</sup>H} NMR (CDCl<sub>3</sub>, δ): 73.2 (s-br, THF-α-CH<sub>2</sub>), 27.75, 27.58, 27.35, 27.19, 27.00, 26.96, 26.90, 26.87 (s, CH<sub>2</sub>-C<sub>5</sub>H<sub>9</sub>), 25.37 (s, THF-β-CH<sub>2</sub>), 24.85, 23.54, 23.21, 22.52, 22.33 (s, CH-C<sub>5</sub>H<sub>9</sub>, 1:2:2:1:1), 1.99 (s, Si(CH<sub>3</sub>)<sub>3</sub>). Anal. Calcd for C<sub>46</sub>H<sub>88</sub>Cl<sub>2</sub>O<sub>14</sub>Si<sub>8</sub>Zr: C, 44.13, H, 7.08. Found: C, 43.84; H, 6.99.

**[(c-C<sub>5</sub>H<sub>9</sub>)<sub>7</sub>Si<sub>7</sub>O<sub>12</sub>]TiCH<sub>2</sub>Ph (**7**).** A red solution of Ti(CH<sub>2</sub>-Ph)<sub>4</sub> (0.88 g, 2.13 mmol) in toluene (25 mL) was cooled to -80 °C and subsequently (c-C<sub>5</sub>H<sub>9</sub>)<sub>7</sub>Si<sub>7</sub>O<sub>9</sub>(OH)<sub>3</sub> (**III**: 1.87 g, 2.14 mmol) was added. The resulting solution was allowed to warm to room temperature and stirred for an additional hour. To remove traces of toluene, the sticky solid was dissolved in hexane (10 mL) and subsequently dried in a vacuum. This procedure was repeated (3×) until a nonsticky product was obtained. Recrystallization from hexane afforded **7** as a yellow powder (1.91 g, 1.89 mmol, 89%). <sup>1</sup>H NMR (benzene-*d*<sub>6</sub>, δ): 7.15 (m, 4H, C<sub>6</sub>H<sub>5</sub>), 6.86 (m, 1H, C<sub>6</sub>H<sub>5</sub>), 2.99 (s, 2H, CH<sub>2</sub>Ph), 1.88 (m, 14H, CH<sub>2</sub>-C<sub>5</sub>H<sub>9</sub>), 1.67 (m, 28H, CH<sub>2</sub>-C<sub>5</sub>H<sub>9</sub>), 1.48 (m, 14H, CH<sub>2</sub>-C<sub>5</sub>H<sub>9</sub>), 1.15 (m, 7H, CH-C<sub>5</sub>H<sub>9</sub>). <sup>13</sup>C{<sup>1</sup>H} NMR (benzene-*d*<sub>6</sub>, δ): 142.92 (*ipso*-C<sub>6</sub>H<sub>5</sub>), 128.65 (C<sub>6</sub>H<sub>5</sub>), 128.59 (C<sub>6</sub>H<sub>5</sub>), 124.32 (C<sub>6</sub>H<sub>5</sub>), 81.53 (t, CH<sub>2</sub>, <sup>1</sup>J<sub>C-H</sub> = 131 Hz), 27.90, 27.87, 27.78, 27.47 (CH<sub>2</sub>-C<sub>5</sub>H<sub>9</sub>), 22.73, 22.65, 22.41 (CH-C<sub>5</sub>H<sub>9</sub>, 3:1:3). <sup>29</sup>Si NMR (toluene, δ): -64.59, -66.55, -67.68 (3:1:3). Anal. Calcd for C<sub>42</sub>H<sub>70</sub>O<sub>12</sub>Si<sub>7</sub>Ti: C, 49.87; H, 6.98. Found: C, 48.66; H, 6.45.

**[(c-C<sub>5</sub>H<sub>9</sub>)<sub>7</sub>Si<sub>7</sub>O<sub>12</sub>]ZrCH<sub>2</sub>Ph (**8**).** At -80 °C, a solution of Zr(CH<sub>2</sub>Ph)<sub>4</sub> (3.05 g, 6.69 mmol) in toluene (30 mL) was added to a suspension of (c-C<sub>5</sub>H<sub>9</sub>)<sub>7</sub>Si<sub>7</sub>O<sub>9</sub>(OH)<sub>3</sub> (5.85 g, 6.68 mmol) in toluene (50 mL). The mixture was allowed to warm to room temperature and subsequently stirred for 1 h. Evaporation of the volatiles yielded crude **8** as a oily yellow solid. To remove traces of toluene, the sticky solid was dissolved in hexane (10 mL) and subsequently dried in a vacuum. Then the product was dissolved in hexane (50 mL) and filtered to remove minor amounts of insoluble impurities. Concentration and cooling to -30 °C gave dimeric **8** (5.2 g, 2.47 mmol, 74%) as pale yellow block-shaped crystals. Recrystallization from hexane at -30 °C afforded crystals suitable for an X-ray structure determination. <sup>1</sup>H NMR (benzene-*d*<sub>6</sub>, δ): 7.47 (d, 2H, C<sub>6</sub>H<sub>5</sub>, <sup>3</sup>J<sub>H-H</sub> = 7 Hz), 7.28 (dd, 2H, C<sub>6</sub>H<sub>5</sub>, <sup>3</sup>J<sub>H-H</sub> = 7 Hz), 6.99 (d, 1H, C<sub>6</sub>H<sub>5</sub>, <sup>3</sup>J<sub>H-H</sub> = 7 Hz), 3.12 (s, 2H, CH<sub>2</sub>C<sub>6</sub>H<sub>5</sub>), 1.7 (m, 50H, C<sub>5</sub>H<sub>9</sub>), 1.2 (m, 6H, C<sub>5</sub>H<sub>9</sub>), 1.1 (m, 4H, C<sub>5</sub>H<sub>9</sub>), 0.8 (m, 3H, C<sub>5</sub>H<sub>9</sub>). <sup>13</sup>C NMR (benzene-*d*<sub>6</sub>, δ): 142.3 (s, *ipso*-C<sub>6</sub>H<sub>5</sub>), 129.9 (d, C<sub>6</sub>H<sub>5</sub>, <sup>1</sup>J<sub>C-H</sub> = 160 Hz), 124.7 (d, C<sub>6</sub>H<sub>5</sub>, <sup>1</sup>J<sub>C-H</sub> = 157 Hz), 57.6 (t, CH<sub>2</sub>C<sub>6</sub>H<sub>5</sub>, <sup>1</sup>J<sub>C-H</sub> = 124 Hz), <sup>13</sup>C{<sup>1</sup>H}: 28.4, 28.1, 27.8, 27.6, 27.5, 27.2, 25.6, 23.6, 23.0, 22.8, 22.6 (s, C<sub>5</sub>H<sub>9</sub>). <sup>29</sup>Si NMR (toluene, 213 K, δ): -57.23, -61.48, -62.05, -62.98, -65.14, -65.57, -67.07. Anal. Calcd for {C<sub>42</sub>H<sub>70</sub>O<sub>12</sub>Si<sub>7</sub>Zr}<sub>2</sub>: C, 47.82; H, 6.69. Found: C, 48.31; H, 7.05.

**[(c-C<sub>5</sub>H<sub>9</sub>)<sub>7</sub>Si<sub>7</sub>O<sub>12</sub>]HfCH<sub>2</sub>Ph (**9**).** A solution of Hf(CH<sub>2</sub>Ph)<sub>4</sub> (1.88 g, 3.46 mmol) in toluene (25 mL) was cooled to -50 °C. Solid (c-C<sub>5</sub>H<sub>9</sub>)<sub>7</sub>Si<sub>7</sub>O<sub>9</sub>(OH)<sub>3</sub> (3.00 g, 3.43 mmol) was added, and

the stirred mixture was allowed to warm to room temperature, yielding a colorless solution. After stirring overnight, the solvent was evaporated, leaving a white solid. To remove traces of toluene, the sticky solid was dissolved in ether (10 mL) and subsequently dried in a vacuum. This procedure was repeated (2×) until a nonsticky product was obtained. The colorless foam obtained was dissolved in hexane (30 mL). Within a few minutes crystals appeared, and after subsequent cooling to -30 °C, dimeric **9** was isolated as a white microcrystalline material (1.70 g, 0.74 mmol, 43%). <sup>1</sup>H NMR (benzene-*d*<sub>6</sub>, δ): 7.43 (d, 2H, *o*-C<sub>6</sub>H<sub>5</sub>, <sup>3</sup>J<sub>H-H</sub> = 7 Hz), 7.28 (t, 2H, *m*-C<sub>6</sub>H<sub>5</sub>, <sup>3</sup>J<sub>H-H</sub> = 7 Hz), 6.87 (t, 1H, *p*-C<sub>6</sub>H<sub>5</sub>, <sup>3</sup>J<sub>H-H</sub> = 7 Hz), 2.63 (s, 2H, Hf-CH<sub>2</sub>), 1.7 (m, 56H, CH<sub>2</sub>-C<sub>5</sub>H<sub>9</sub>), 1.2 (m, 6H, CH-C<sub>5</sub>H<sub>9</sub>), 0.9 (m, 1H, CH-C<sub>5</sub>H<sub>9</sub>). <sup>13</sup>C{<sup>1</sup>H} NMR (benzene-*d*<sub>6</sub>, δ): 148.24 (s, *ipso*-C<sub>6</sub>H<sub>5</sub>), 128.5 (s, C<sub>6</sub>H<sub>5</sub>), 128.07 (s, C<sub>6</sub>H<sub>5</sub>), 122.26 (s, C<sub>6</sub>H<sub>5</sub>), 65.39 (t, Hf-CH<sub>2</sub>, <sup>1</sup>J<sub>C-H</sub> = 112 Hz), 28.26, 28.05, 27.85, 27.73, 27.47 (s, CH<sub>2</sub>-C<sub>5</sub>H<sub>9</sub>), 23.67, 22.90, 22.51 (s, CH-C<sub>5</sub>H<sub>9</sub>, 3:3:1). Anal. Calcd for {C<sub>42</sub>H<sub>70</sub>HfO<sub>12</sub>Si<sub>7</sub>}<sub>2</sub>: C, 44.17; H, 6.18. Found: C, 43.77; H, 6.30.

**[(c-C<sub>5</sub>H<sub>9</sub>)<sub>7</sub>Si<sub>7</sub>O<sub>12</sub>]ZrCH<sub>2</sub>Ph·2THF (**10**).** Zr(CH<sub>2</sub>Ph)<sub>4</sub> (0.95 g, 2.08 mmol) was dissolved in THF (20 mL) and cooled to -90 °C. Then, solid (c-C<sub>5</sub>H<sub>9</sub>)<sub>7</sub>Si<sub>7</sub>(OH)<sub>3</sub> (1.82 g, 2.08 mmol) was added, and the mixture was slowly warmed to room temperature. The solvent of the pale yellow solution was evaporated, and the crude product was dried thoroughly and extracted (30 mL) with hexane. Concentration and cooling to 4 °C afforded **10** as colorless crystals (0.90 g, 0.75 mmol, 36%). <sup>1</sup>H NMR (benzene-*d*<sub>6</sub>, δ): 7.25 (m, 4H, C<sub>6</sub>H<sub>5</sub>), 6.86 (m, 1H, C<sub>6</sub>H<sub>5</sub>), 3.94 (s (br), 8H, THF-α-CH<sub>2</sub>), 2.17 (s, 2H, CH<sub>2</sub>Ph), 1.95, 1.81, 1.72, 1.58, 1.51 (m, 56H, CH<sub>2</sub>-C<sub>5</sub>H<sub>9</sub>), 1.44 (s (br), 8H, THF-β-CH<sub>2</sub>), 1.21, 1.06, 0.89 (m, 7H, CH-C<sub>5</sub>H<sub>9</sub>). <sup>13</sup>C NMR (benzene-*d*<sub>6</sub>, δ): 152.74 (s, *ipso*-C<sub>6</sub>H<sub>5</sub>), 128.16 (d, C<sub>6</sub>H<sub>5</sub>, <sup>1</sup>J<sub>C-H</sub> = 158 Hz), 126.26 (d, C<sub>6</sub>H<sub>5</sub>, <sup>1</sup>J<sub>C-H</sub> = 159 Hz), 119.31 (d, C<sub>6</sub>H<sub>5</sub>, <sup>1</sup>J<sub>C-H</sub> = 151 Hz), 71.02 (t, THF-α-CH<sub>2</sub>, <sup>1</sup>J<sub>C-H</sub> = 146 Hz), 54.21 (t, CH<sub>2</sub>Ph, <sup>1</sup>J<sub>C-H</sub> = 117 Hz), 28.37, 27.99, 27.86, 27.55, 27.52, 27.42 (t, CH<sub>2</sub>-C<sub>5</sub>H<sub>9</sub>, <sup>1</sup>J<sub>C-H</sub> = 129 Hz), 25.30 (t, THF-β-CH<sub>2</sub>, <sup>1</sup>J<sub>C-H</sub> = 133 Hz), 23.80, 23.17, 22.89 (d, CH-C<sub>5</sub>H<sub>9</sub>, <sup>1</sup>J<sub>C-H</sub> = 117 Hz). <sup>29</sup>Si NMR (THF, δ): -66.62, -66.74, -68.40 (3:1:3). The crystalline product gradually lost THF. Therefore no satisfactory elemental analysis could be obtained.

**Hydrogenation of 1-Hexene.** Hydrogenation of 1-hexene was carried out in pressure NMR tubes containing toluene solutions of 40–60 μmol of the precursor (**7**–**10**) and 1 mmol of 1-hexene under 4 atm of dihydrogen. For **8** and **9**, after 10–20 h at 75 °C toluene was quantitatively formed and all the 1-hexene was selectively hydrogenated to *n*-hexane. In the case of **7** and **10**, no observable reaction had occurred under the same conditions.

**NMR Tube Reaction of **8** with B(C<sub>6</sub>F<sub>5</sub>)<sub>3</sub>.** NMR tubes were charged with toluene-*d*<sub>8</sub> solutions of **8** (75–95 mg, 70–90 μmol) and variable quantities (1, 2, and 10 equiv) of B(C<sub>6</sub>F<sub>5</sub>)<sub>3</sub>. The reactions were followed by <sup>1</sup>H, <sup>11</sup>B, and <sup>19</sup>F NMR. The NMR (<sup>1</sup>H, <sup>11</sup>B, <sup>19</sup>F) spectra recorded within 5 min after the addition of 1 equiv of B(C<sub>6</sub>F<sub>5</sub>)<sub>3</sub> to a toluene-*d*<sub>8</sub> solution of **8** showed the instantaneous formation of a new zirconium benzyl complex (ZrCH<sub>2</sub> = 2.73 ppm) and [PhCH<sub>2</sub>B(C<sub>6</sub>F<sub>5</sub>)<sub>3</sub>]<sup>-</sup> as the only boron product (<sup>1</sup>H, BCH<sub>2</sub> = 3.52 ppm, <sup>11</sup>B, PhCH<sub>2</sub>B(C<sub>6</sub>F<sub>5</sub>)<sub>3</sub> = -16.7 ppm). <sup>19</sup>F NMR indicates that this borate anion is not coordinated to the cationic zirconium complex: Δδ(F<sub>m</sub> - F<sub>p</sub>) = 2.59 ppm. Within 30 min at 50 °C, the cationic complex has decomposed to unidentified product(s). When treated with 2 or 10 equiv of B(C<sub>6</sub>F<sub>5</sub>)<sub>3</sub>, complex **8** still reacted with only 1 equiv of B(C<sub>6</sub>F<sub>5</sub>)<sub>3</sub>, leaving the excess borane untouched.

**Ethylene Polymerization Experiments.** Ethylene polymerization experiments were carried out in a 1.3 L DSM stainless steel reactor equipped with a stationary steel stirrer. In a typical experiment, under nitrogen PMH (pentamethylheptane, 600 mL) was brought into the reactor. The reactor was heated under stirring to the required temperature. Additionally, a constant ethylene pressure was maintained. A toluene (10 mL) solution of the cocatalyst was syringed into

a 100 mL catalyst dosing vessel containing PMH (25 mL). Subsequently, the solution was transferred into the reactor. After 15 min, the desired amount of catalyst precursor was introduced into the reactor in the same way, after which the catalyst dosing vessel was washed automatically with PMH ( $2 \times 50$  mL). The polymerization reactions were carried out under isothermal conditions and constant ethene pressure. At the end of the reaction, the reaction mixture was collected and quenched with 20 mL of methanol. Antioxidant (Irganox 1076) was added to stabilize the polymer. The polymer was dried under vacuum at 70 °C for 24 h. If possible, the obtained polymer was analyzed by SEC-DV (weight-averaged molecular weight ( $M_w$ ) and molecular weight distribution (MWD)).

**X-ray Structure Determination of  $[(\text{C-C}_5\text{H}_9)_7\text{Si}_7\text{O}_{11}(\text{OSiMe}_3)_2]\text{Zr}\cdot 2\text{THF}$  (**5**) and  $[(\text{C-C}_5\text{H}_9)_7\text{Si}_7\text{O}_{12}]\text{ZrCH}_2\text{C}_6\text{H}_5$  (**8**).** Suitable crystals were measured at 130 K with graphite-monochromated Mo K $\alpha$  radiation on an Enraf-Nonius CAD-4F diffractometer equipped with a low-temperature unit.<sup>31</sup> Precise lattice parameters and their standard deviation and orientation matrix were derived from the angular settings of 22 reflections (**5**,  $18.21^\circ < \theta < 20.41^\circ$ ; **8**,  $18.07^\circ < \theta < 20.57^\circ$ ) in four alternative settings.<sup>32</sup> The unit cell was identified as monoclinic (space group  $P2_1/c$ ) for **5** and triclinic (space group  $P\bar{1}$ ) for **8**.<sup>33</sup> Intensity data were corrected for Lorentz and polarization effects and scale variation and reduced to  $F_o^2$ .<sup>34</sup> The structures were solved by Patterson methods, and extension of the model was accomplished by direct methods applied to difference structure factors using the program DIRDIF.<sup>35</sup>

(30) (a) Zucchini, U.; Albizzati, E.; Giannini, U. *J. Organomet. Chem.* **1971**, *26*, 357. (b) Wngrovius, J. H.; Schrock, R. R.; *J. Organomet. Chem.* **1981**, *305*, 319.

(31) Van Bolhuis, F. *J. Appl. Crystallogr.* **1971**, *4*, 263.

(32) De Boer, J. L.; Duisenberg, A. J. M. *Acta Crystallogr.* **1984**, *A40*, C410.

(33) No higher metric lattice symmetry or extra metric symmetry elements were found: (a) Spek, A. L. *J. Appl. Crystallogr.* **1988**, *21*, 578. (b) Le Page, Y. *J. Appl. Crystallogr.* **1987**, *20*, 264. (c) Le Page, Y. *J. Appl. Crystallogr.* **1988**, *21*, 983.

(34) Spek, A. L. *HELENA Program for Data Reduction*; University of Utrecht: Utrecht, The Netherlands, 1993.

(35) Beurskens, P. T.; Beurskens, G.; Bosman, W. P.; de Gelder, R.; García-Granda, S.; Gould, R. O.; Israël, R.; Smits, J. M. M. *The DIRDIF-97 program system*; Crystallography Laboratory, University of Nijmegen: Nijmegen, The Netherlands, 1992.

The positional and anisotropic thermal displacement parameters for the non-hydrogen atoms were refined on  $F^2$  with full-matrix least-squares procedures minimizing the function  $Q = \sum_h [w(|F_o^2 - kF_c^2|)^2]$ , where  $w = 1/[\sigma^2(F_o^2) + (aP)^2 + bP]$ ,  $P = [\max(F_o^2, 0) + 2F_c^2]/3$ ,  $F_o$  and  $F_c$  are the observed and calculated structure factor amplitudes, respectively;  $a$  and  $b$  were refined. Reflections were stated observed if satisfying  $F^2 > 0$  criterion of observability. For **5**, a subsequent Fourier synthesis showed some electron density (not exceeding  $2.9 \text{ e}/\text{\AA}^3$ ) in the holes of the lattice which could be correlated to partly occupied and disordered solvent molecules of THF. Using the BYPASS procedure, the amount of THF was found to be 0.72 per molecule of **5**. For both **5** and **8** refinement was complicated by conformational disorder of the cyclopentyl substituents. Final refinement on  $F^2$  was carried out by full-matrix least-squares techniques. Neutral atom scattering factors and anomalous dispersion corrections were taken from *International Tables of Crystallography*.<sup>36</sup> All calculations were carried out at a HP9000/735 computer at the University of Groningen with the program packages *SHELXL*,<sup>37</sup> *PLATON*,<sup>38</sup> and *ORTEP*.<sup>39</sup>

**Acknowledgment.** We wish to thank DSM Research B.V. for funding this research. We also thank Dr. A. J. R. L. Hulst, University of Twente, The Netherlands, for measuring the  $^{19}\text{F}$  NMR spectra.

**Supporting Information Available:** Tables of atomic coordinates, thermal displacement parameters, bond lengths, bond angles, and torsion angles for **5** and **8** (34 pages). Ordering information is given on any current masthead page.

OM980687K

(36) *International Tables of Crystallography*, Vol. C.; Wilson, A. J. C., Ed.; Kluwer Academic Publishers: Dordrecht, The Netherlands, 1992.

(37) Scheldrick, G. M. *SHELX-97. Program for the Solution and Refinement of Crystal Structures*; University of Göttingen: Göttingen, Germany, 1997.

(38) Spek, A. L. *PLATON. Program for the Automated Analysis of Molecular Geometry*; University of Utrecht: Utrecht, The Netherlands, 1996.

(39) Johnson, C. K. *ORTEP II*. Report ORNL-5138; Oak Ridge National Laboratory: Oak Ridge, TN, 1976.